

# Rationale for Tailoring an Alternative Oncology Trial Using a Novel Gallium-Based Nanocomplex: Mechanistic Insights and Preclinical Challenges

Technology in Cancer Research & Treatment  
Volume 21: 1-20  
© The Author(s) 2022  
Article reuse guidelines:  
sagepub.com/journals-permissions  
DOI: 10.1177/15330338221085376  
journals.sagepub.com/home/tct  


Nihal Mostafa, MSc<sup>1</sup> , Ahmed Salem, PhD<sup>1</sup>,  
Somaya Z. Mansour, PhD<sup>2</sup>, Sawsan M. El-Sonbaty, PhD<sup>3</sup>,  
Fatma S. M. Moawed, PhD<sup>4</sup>, and Eman I. Kandil, PhD<sup>1</sup>

## Abstract

**Introduction:** In the fight against cancer, cisplatin is most widely used as a clinical mainstay for the chemotherapy of various human cancers. Meanwhile, its cytotoxic profile, as well as drug resistance, limits its widespread application. The goal of precision medicine is to tailor an optimized therapeutic program based on the biology of the disease. Recently, nanotechnology has been demonstrated to be promising in this scenario. **Objective:** The current work provides a rationale for the design of an alternative oncology trial for the treatment of hepatocarcinogenesis using a novel eco-friendly nanocomplex, namely gallic acid-coated gallium nanoparticles. Moreover, the study tests whether the antineoplastic efficacy of gallic acid-coated gallium nanoparticles could be enhanced or not when it is administered together with cisplatin. **Methods:** The work comprised a series of both *in vitro* and *in vivo* investigations. The *in vivo* therapeutic efficacy of such treatments, against diethylnitrosamine-induced hepatocarcinogenesis, was strictly evaluated by tracking target genes expressions, iron homeostasis, diverse biomarkers alterations, and lastly, routine paraclinical investigations were also assessed. **Results:** The *in vitro* biological evaluation of gallic acid-coated gallium nanoparticles in a HepG-2 cancer cell line established its superior cytotoxicity. Else more, the results of the *in vivo* experiment highlighted that gallic acid-coated gallium nanoparticles could diminish key hallmarks of cancer by ameliorating most of the investigated parameters. This was well-appreciated with the histopathological findings of the liver architectures of the treated groups. **Conclusions:** Our findings suggest that novel biogenic Ga-based nanocomplexes may potentially present new hope for the development of alternative liver cancer therapeutics, which should attract further scientific interest.

## Keywords

hepatocarcinogenesis, cisplatin (CDDP), gallic acid (GA), gallium (Ga), green nanotechnology

## Abbreviations

AFP, alpha-fetoprotein; ALP, alkaline phosphatase; ALT, alanine transferase; AST, aspartate transferase; cDNA, complementary DNA; DEB-TACE, doxorubicin-eluting beads transarterial chemoembolization; DLS, dynamic light scattering; FTIR, Fourier-transform infrared spectroscopy; GA, gallic acid; GSH, glutathione; HCC, hepatocellular carcinoma; H&E, hematoxylin and eosin; IL, interleukin; LPO, lipid peroxidation; MDA, malondialdehyde; MDR, multicellular drug resistance; RR, ribonucleotide reductase; RT-PCR, real-time polymerase chain reaction; RT, room

<sup>1</sup> Department of Biochemistry, Faculty of Science, Ain Shams University, Cairo, Egypt

<sup>2</sup> Radiation Biology, National Center for Radiation Research and Technology (NCRRT), Atomic Energy Authority (AEA), Cairo, Egypt

<sup>3</sup> Radiation Microbiology, National Center for Radiation Research and Technology (NCRRT), Atomic Energy Authority (AEA), Cairo, Egypt

<sup>4</sup> Health Radiation Research, National Center for Radiation Research and Technology (NCRRT), Atomic Energy Authority (AEA), Cairo, Egypt

## Corresponding Author:

Nihal Mostafa, Department of Biochemistry, Faculty of Science, Ain Shams University, Cairo 13987, Egypt.

Email: [nihalbiochemist@sci.asu.edu.eg](mailto:nihalbiochemist@sci.asu.edu.eg)



temperature; SOD, superoxide dismutase; TEM, transmission electron microscopy; TIBC, total iron binding capacity; VEGF, vascular endothelial growth factor.

Received: August 27, 2021; Revised: February 7, 2022; Accepted: February 11, 2022.

## Introduction

Hepatocellular carcinoma (HCC) is one of the most common and lethal malignant tumors worldwide.<sup>1,2</sup> The incidence of liver cancer and mortality shows a stable increase globally. An estimated incidence of primary liver cancer ranges from 600 000 to 800 000 annually, accounting for 5.6% of all human cancers and projected cases of about 1 million by 2030.<sup>3</sup> At present, limited treatment options with marginal clinical benefits are available. Traditionally, curative treatment options for early-stage HCC include surgical resection, radiofrequency ablation, transarterial chemoembolization, liver transplantation, and rarely systemic chemotherapy.<sup>4</sup> Nevertheless, the main drawbacks of curative treatment are recurrence of HCC, which leads to an incidence of more than 70% at 5 years.<sup>5</sup> Moreover, systemic chemotherapies particularly in the form of conventional cytotoxic drugs are generally ineffective with low survival benefits,<sup>6</sup> as the patients fail to withstand the trials of new chemotherapeutic agents due to underlying liver dysfunction. Hence, there is an urgent need for developing more specific and effective alternative treatment strategies than cytotoxic chemotherapy. In recent years, molecular targeted therapy based on the molecular pathways that lead to carcinogenic mechanisms of HCC is a novel and promising treatment approach.<sup>7</sup> In recent years, nano-based therapy has advanced to cancer treatment with new procedures in order to solve and reduce the limitations of current cancer treatments.<sup>8</sup> These nanosystems are able to control the release of drugs and can significantly increase the cytotoxic effect of anticancer drugs in specific target sites.<sup>9</sup> Moreover, advances in nanotechnology have also improved the rapid and sensitive detection of cancer biomarkers.<sup>8</sup>

Within the last 2 decades, the exponential increase in published papers that have dealt with the use of chemotherapeutic-based nanoparticles (NPs) for liver cancer treatment indicates the promising prospects of nanotechnology in improved clinical liver cancer management.<sup>10,11</sup> Many NP formulations of anticancer drugs are approved for human use and are already available in the market.<sup>12,13</sup> In the HCC field, there is only one nanodrug clinically approved in Europe and Asia, the doxorubicin-eluting beads transarterial chemoembolization (DEB-TACE). Compared to the conventional TACE, this technology exerts both the therapeutic components of TACE, namely the drug carrier function and embolization, thus minimizing the risk of the systemic drug.<sup>14</sup> Despite promising results of doxorubicin DEB-TACE, it is necessary to conduct clinical trials to overcome the potential limitation of TACE with small-caliber DEBs.<sup>15</sup> Hence, alternative novel nanotechnologies are currently being investigated in clinical trials.<sup>1</sup>

Outstandingly, nanotechnology provides a new approach to synthesize new metal-containing anticancer agents.<sup>16</sup>

Nanoparticles made of non-noble metals such as gallium (Ga) have recently attracted significant attention due to promising applications.<sup>17</sup> Gallium nitrate is a first generation of Ga compounds that had anticancer property in human beings. In phase II medical trials, vast responses to gallium nitrate have been seen in patients whose tumors had relapsed or failed to reply to conventional chemotherapy. Newer Ga forms combined with therapeutic strategies are a strategy to improve the results of the treatment.<sup>18</sup> Indeed, scientists are investigating Ga complexes as small molecules or NPs for targeted drug delivery.<sup>19</sup> Recent studies demonstrated that aqueous dispersions of GaNPs exhibit antitumor properties both *in vitro* and *in vivo*, with low cytotoxicity to normal cells.<sup>20</sup> Shedding the light into the mode of antineoplastic action of GaNPs, the iron-mimicking ability of Ga allows its interaction with important iron-dependent biological processes.<sup>21</sup> Accordingly, Ga competes with and substitute for Fe<sup>+3</sup> in the active site of ribonucleotide reductase (RR), thus inhibiting this enzyme crucial for DNA synthesis.<sup>22</sup> Moreover, the non-iron targets for Ga are somewhat diverse. Strictly, both iron targeting and non-iron targeting mechanistic insights act in concert to enhance its potency as an antineoplastic agent.<sup>23</sup> Over and above, Ga compounds have been demonstrated to be active against multicellular drug resistance (MDR) in cancer cells which remains a major obstacle to the successful treatment of cancer.<sup>24</sup> In conclusion, GaNPs may constitute a promising alternative agent for cancer therapeutics in the near future. However, more studies are needed to elucidate the full cellular mechanisms of GaNPs action for the treatment of cancer with higher effectiveness and lower cost.<sup>20</sup> At the interface of HCC, RRM<sub>2</sub> (the M<sub>2</sub> subunit of RR) is located in a region (1q:163) of frequent cytogenetic aberration in HCC, suggesting it to be a chemotherapeutic target in HCC. Based on <sup>67</sup>Ga scans, Ga is known to accumulate in HCC tumors, and because RR is generally highly overexpressed by HCC cells, a compelling rationale exists for exploring the potential utility of Ga in treating HCC.<sup>22</sup> In this connection, former biogenic Ga-based NPs with preclinical antitumor activity have been recently tested against chemically induced HCC and its consequent metastasis.<sup>18,25</sup>

For analytical applications, research is required into the development of protocols for synthesis and functionalization of these NPs.<sup>8</sup> A possible turning point could be the use of targeting agents covalently bound to particle surface; this approach demonstrated a superior therapeutic effect in different animal models. Recent studies have individuated several molecules that can represent possible targets for the selective delivery of targeted NPs. This probably represents the next step in nanomedicine for the treatment of HCC.<sup>1</sup> In this connection, the rationale for preparing bioactive Ga (III) complexes with different organic ligands could be an excellent approach to circumvent cell resistance to Ga and improve its bioavailability.

The organic ligands may be useful carriers of Ga into the cells. Noteworthy, these organometallic complexes would in principle exhibit effects due to the synergistic actions from the metal and ligand components assembled in one compound.<sup>26</sup> Nanoparticles produced by a biogenic enzymatic process could be the answer, which provides a new approach to synthesize new metal-containing agents by combining organic ancillary ligands to the candidate metalcore at the nanoscale.<sup>20</sup> The later pleasant bio-inspired nanofabrication technique is called “green synthesis” of NPs, representing a road map to safer nanomaterials.

Natural products are a valuable source of anticancer agents, representing an important alternative remedy for cancer in the 21st century.<sup>27</sup> Gallic acid (GA) is a natural bioactive polyphenolic compound isolated from plant derivatives and fruits.<sup>28</sup> It is the chief antioxidant component responsible for the efficient antiradical and anticancer properties of a number of plant extracts.<sup>29</sup> Accordingly, it has been reported to show anticancer effects against various cancers.<sup>28</sup> In the context of HCC, GA was capable of selectively inhibiting the proliferation of HepG2 and SMMC-7721 human HCC cells *in vitro* in a time- and dose-dependent manner.<sup>30</sup> Moreover, methyl gallate, a GA-derived compound, inhibited HCC proliferation both *in vitro* and *in vivo* through increasing ROS production and apoptosis.<sup>31</sup> On the plus side, GA has been reported to be a potent antiproliferative agent against diethylnitrosamine (DEN)-induced HCC owing to its affinity to regulate signal transducer and activator of transcription 3 signaling pathway.<sup>32,33</sup> Consequently, GA may possess the potential to be a novel therapeutic compound for use in the treatment of HCC. Noteworthy, GA is hydrophilic, causing it difficult to penetrate the wall of cancer cells.<sup>34</sup> This issue has been resolved by using nanotechnology. Nanoparticles can be used as nano-carriers for antioxidants and such NPs that are termed as nano-antioxidants.<sup>35</sup> Accordingly, preparation of GA in form of NPs is believed to increase its hydrophobicity to be able to diffuse easily through the cancer cell membrane and hence, improve its anticancer activity.<sup>34</sup> Gallic acid exerts its anticarcinogenic effects through a pleiotropic molecular mechanism(s) of action on cell cycle, cell apoptotic processes, angiogenesis, and metastasis.<sup>36</sup> Nonetheless, the primary mechanism of action of GA is attributed to both its antioxidant as well as prooxidant characteristics, displaying a dual-edge sword behavior.<sup>29</sup> Thus, GA could be considered as an attractive candidate and/or a starting point for the development of novel anticancer agents.<sup>37</sup>

Gracefully written, developing new cancer therapies is an ever-pressing passion that inspired us towards the world of alternative cancer therapies in which conventional treatments and innovative targeted therapies work hand in hand to improve the therapeutic outcome. The next section will provide the rationale for the design of an alternative oncology trial aiming at fighting hepatocarcinogenesis, using a novel biogenic Ga-based nanocomplex that has been currently developed and evaluated for its antineoplastic activity. Beyond this, our hope is pinned on tailoring an optimized preclinical therapeutic program based on the biology of the disease, and further the evolutionary principles of tumor development.

## Materials and Methods

### Chemicals

Diethylnitrosamine and  $\text{Ga}(\text{NO}_3)_3$  were purchased from Sigma-Aldrich. CDDP was purchased from Oncotec Pharma Production GmbH, MYLAN. All other chemicals and reagents used were of pure analytical grade.

### Cell Line

A Human hepatocellular cancer (HepG-2) cell line was obtained from the American Type Culture Collection (ATCC). Cells were cultured in RPMI 1640 medium complemented with 10% FBS at 37 °C in a humidified atmosphere with 5%  $\text{CO}_2$ . N.B. The HepG2 cell line was strictly selected in the existing study to justify the possible *in vitro* cytotoxic effect of gallic acid-coated gallium nanoparticles (GA-GaNPs) on cancerous hepatocytes.

### Experimental Animals

Adult male Swiss albino rats weighing (100-120 g) b.wt. were purchased from the breeding unit of Nile Company for Pharmaceuticals and Chemical Industries. The animals were randomly housed in appropriate steel mesh cages (8 rats/cage) which were kept under standard laboratory conditions. The animals were maintained on starter poultry pellets and water *ad libitum* for one week before starting the experiment as an acclimatization period. Animal maintenance and treatments were conducted in accordance with International Guiding Principles, as approved by Research Ethics Committee in National Center for Research and Technology (REC-NCRRT). The Guide for the Care and Use of Laboratory Animals: Eighth Edition has been used to assist in the adequate standard care of the animals and using animals in ways judged to be scientifically, technically, and humanely appropriate.<sup>38</sup> The reporting of this study conforms to ARRIVE 2.0 guidelines.<sup>39</sup> The G-power calculation was done for estimating the sample size decided for the study. Indeed, efforts have been made to minimize the number of animals utilized in this study, and further decrease their suffering. There were no inclusion and/or exclusion criteria for this study.

## Methods

### Chemical Studies

*Gallic acid-mediated greener nanosynthesis of gallium-based nanoparticles.* Gallium NPs protected by GA were synthesized referring to the methods of Li *et al.*<sup>40</sup> with certain modifications. Both  $\text{Ga}(\text{NO}_3)_3$  and GA were freshly used. Following the principles of green synthesis of NPs, ultrapure water was used as an environmentally benign solvent over the course of the production and storage of GA-GaNPs. First, 20 mM of  $\text{Ga}(\text{NO}_3)_3$  was prepared in double-distilled water under magnetic stirring at room temperature (RT). Then, 10 mM of GA was added, and the pH value was adjusted to 11.0 with 1.0 M NaOH. Subsequently, the reaction was maintained at RT for 30 min. Visual observation was conducted periodically to check for

NPs formation. The developed nanoproduct (GA-GaNPs) was then condensed and purified by centrifugation at (15 000 × g) for 10 min and washed with double-distilled water 3 times.

**Physicochemical characterization of GA-GaNPs.** A panel of physicochemical analyses was conducted at the Nanotechnology Unit, Egyptian Petroleum Institute (Egypt), for nano-verification of the novel grown NPs, including: (1) Transmission electron microscopy (TEM): The morphology and size of GA-GaNPs were determined from TEM micrographs of JEOL Model 1200EX. The software (Advanced Microscopy Techniques) for the digital TEM camera was calibrated for size measurement of the NPs.<sup>41</sup> (2) Dynamic light scattering (DLS): The size distribution and Z (zeta) potential of the GA-GaNPs were measured with a Malvern Zetasizer nano ZS® (Ver 6.32), United Kingdom. (3) Fourier-transform infrared spectroscopy (FTIR): The analysis was performed on a VERTEX 70/70v FTIR spectrometer (Bruker), and recorded over cumulative scans in the wave number between 4000 and 400 cm<sup>-1</sup>. (4) Ultraviolet-visible (UV-Vis) spectroscopy: Spectrum absorbance of GA-GaNPs was analyzed by JASCO UV-Vis spectrophotometer model V-750 in a measurement range of 200 to 800 nm.

### Biochemical Studies

The present study was designed to comprise a series of both *in vitro* and *in vivo* investigations as follows.

#### *In vitro* study

**Cytotoxicity assay.** Cytotoxicity of both GA-GaNPs and CDDP on HepG2 cells was evaluated by a thiazolyl blue tetrazolium bromide (MTT) assay based on the mitochondrial dehydrogenase conversion of the MTT into blue formazan crystals in the viable cells.<sup>42</sup>

#### *In vivo* studies

**Acute toxicity study.** Determination of the lethal dose of GA-GaNPs, as a newly synthesized drug, is an essential initial step in the *in vivo* evaluation of the toxic characteristics of the drug and provides information on health hazards likely to arise from short-term exposure to it. A total of 24 male Swiss albino rats was divided into 4 groups and intraperitoneally (*i.p.*) administered GA-GaNPs in elevated doses ranging from 25 to 250 mg/kg b.wt. Mortality incidence was recorded in 1 to 7 days after administration.

#### Evaluation of antineoplastic efficacy

**Chemical induction of hepatocarcinogenesis.** An experimental model of chemical hepatocarcinogenesis in male Swiss albino rats was induced by receiving a daily *i.p.* dose of 20 mg/kg b.wt. of DEN diluted in normal saline (0.9%) for 6 weeks, according to the method of Darwish and El-Boghdady,<sup>43</sup> with some modifications.

**Experimental design.** A total of 80 male Swiss albino rats was randomly distributed (simple randomization) into 8 equal

groups (n=10) and categorized as follows. (1) Control: Normal healthy rats, (2) GA-GaNPs: Rats were injected with a daily *i.p.* dose of GA-GaNPs (25 mg/kg b.wt.) for one month. (3) CDDP: Rats were *i.p.* administered CDDP in a daily dose of (1 mg/kg b.wt.), according to Chen *et al.*,<sup>44</sup> for one month. (4) GA-GaNPs + CDDP: Rats were daily *i.p.* injected with GA-GaNPs together with CDDP during the treatment month. (5) DEN-model: Rats in this group received DEN in a dose of 20 mg/kg b.wt., 5 times a week for 6 weeks. (6) DEN + GA-GaNPs: After 6 weeks of DEN treatment, animals were treated with GA-GaNPs. (7) DEN + CDDP: After DEN-intoxication, animals were treated with CDDP. (8) DEN + GA-GaNPs + CDDP: DEN-intoxicated animals were treated with GA-GaNPs together with CDDP.

**Sample collection.** At the end of 10 weeks, animals in all groups were fasted overnight prior to euthanizing *via* exsanguination. Firstly, animals were anesthetized by (1.5%-2%) isoflurane inhalation. And then, blood samples were obtained by heart puncture and collected in sterile heparinized and non-heparinized tubes. Livers of each group were quickly excised, perfused with cold isotonic saline, dried, and divided into 2 portions; the first portions were fixed in 10% formalin for histological examination, whereas the second portion was snap-frozen directly in liquid nitrogen and stored at -80 °C prior to RNA isolation for gene expression analyses.

**Biochemical analyses.** A panel of biochemical analyses was performed on plasma and/or liver homogenate samples to track 4 axes-mechanistic aspects including; (1) Gene expression aspects presented by precisely quantifying relative expression levels of cytochrome c (*Cyt-c*), *C-Myc* oncogene, and heat shock protein-70 (*HSP-70*) target genes using real-time polymerase chain reaction (RT-PCR). Total RNA was harvested from liver tissue samples using SV-total RNA isolation system (Promega). Then, complementary DNA (cDNA) was synthesized using the superscript choice system high-capacity cDNA reverse transcription kit (Life Technologies). Finally, RT-PCR was performed by SYBR

**Table 1.** List of Designed Primers for RT-PCR.

Gene symbol	Primer sequence (5'-3')
<i>Cyt-c</i>	F: 5'-GGC TGC AGT GTA GCT GTG AT-3' R: 5'-GAT GGA GTT TCC TTT ATC TGT TGC-3'
<i>Hsp70</i>	F: 5'-TTG TCC ATG TTA AGG TTT TGT GGT ATA-3' R: 5'-GTT TTT TTC ATT AGT TTG TAG TGA TGC AA-3'
<i>C-Myc</i>	F: 5'-GAG GAG AAA CGA GCT GAA GCG TAG-3' R: 5'-TTC TCG CCG TTT CCT CAG TAA GTC-3'
<i>GAPDH</i>	F: 5'-CAC CCT GTT GCT GTA GCC ATA TTC-3' R: 5'-GAC ATC AAG AAG GTG GTG AAG CAG-3'

Abbreviation: RT-PCR, real-time polymerase chain reaction.

Green PCR Master Mix together with specific primers using an Applied Biosystem with software v1.7. The sequence of the primers used for RT-PCR is listed in Table 1. Data from real-time assays were quantified using the v1.7 sequence detection software from PE Biosystems. Target gene expression levels were normalized to the GAPDH house-keeping gene. Fold change in mRNA expression was measured using the comparative cycle threshold ( $2^{-\Delta\Delta C_t}$ ) method. (2) Iron mimicry aspects verified by monitoring iron ( $Fe^{+2}$ ) and total iron binding capacity (TIBC), using BioVision's assay kits (Catalog # K390 & K392-100, respectively), (3) Biological markers aspects elucidated by tracking; (a) Tumorigenic marker (alpha-fetoprotein, AFP) using a rat AFP ELISA kit purchased from Cusabio Biotech Co., Ltd. (USA), (b) Apoptotic marker (caspase-9, CASP9) using rat CASP9 ELISA kit purchased from Novus Biologicals Co., Ltd. (USA), (c) Angiogenic marker (vascular endothelial growth factor, VEGF) using a rat VEGF ELISA kit purchased

from R&D Systems Europe, Ltd, (d) Oxidative stress biomarkers involved assessment of reduced glutathione (GSH) according to Beutler,<sup>45</sup> superoxide dismutase (SOD) according to Nishikimi *et al.*<sup>46</sup> and catalase (CAT) based roughly on the methods of Aebi,<sup>47</sup> and Fossati *et al.*<sup>48</sup> and (e) Lipid peroxidation (LPO) marker; malondialdehyde (MDA) was quantified according to the method of Ohkawa *et al.*<sup>49</sup> as well as (4) Routine paraclinical aspects monitored by the colorimetric assessment of a panel of liver and kidney damage biomarkers involving albumin (Alb) based on the method described by Doumas *et al.*<sup>50</sup>, total bilirubin (T.Bil) according to the method described by Walter and Gerade,<sup>51</sup> alkaline phosphatase (ALP) activity based on the method of Belfield and Goldberg,<sup>52</sup> and activities of alanine transferase (ALT) and aspartate transferase (AST) according to the method of Reitman and Frankel.<sup>53</sup> Additionally, creatinine (Cr) and urea were also colorimetrically assessed using commercial kits purchased from Diamond Company, Egypt.

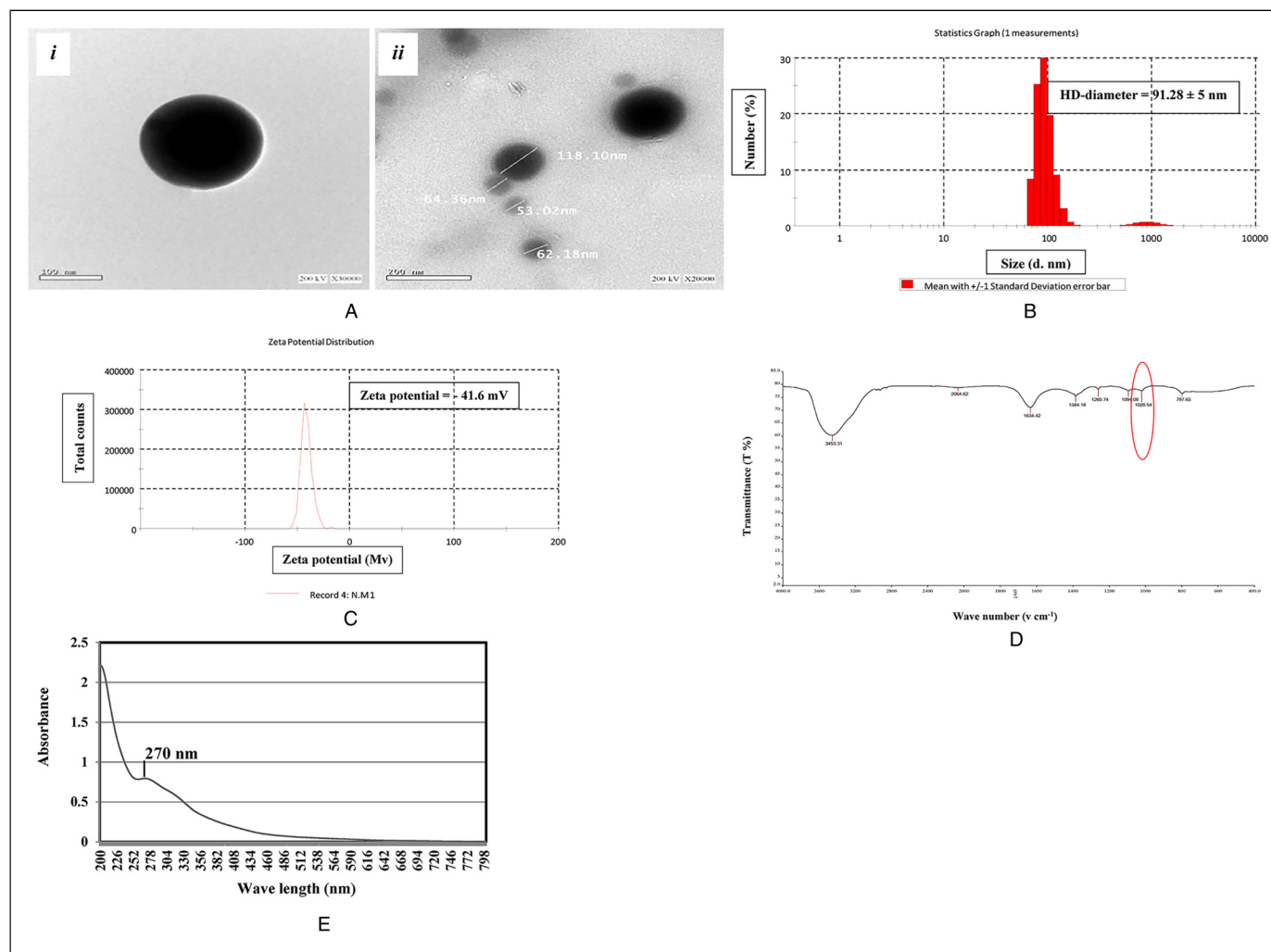


**Figure 1.** (A) Transmission electron microscopy (TEM) images of gallic acid-coated gallium nanoparticles (GA-GaNPs; Magnification =  $\times 30\,000$  &  $\times 20\,000$ ; Scale bar = 100 nm & 200 nm). (B) Size statistics graph of gallic acid-coated gallium nanoparticles (GA-GaNPs). (C) Zeta potential distribution of GA-GaNPs. (D) Fourier-transform infrared spectroscopy (FTIR) spectrum of GA-GaNPs. (E) UV-Vis absorption spectrum of GA-GaNPs.

## Histopathological Survey

Liver tissue biopsies were fixed in 10% formalin for 24 h, then standard dehydration and paraffin-wax embedding procedures were performed. Sections of 5  $\mu\text{m}$  thickness were cut in a slide microtome, adhered to glass slides, deparaffinized, and stained by hematoxylin and eosin stains (H&E) for routine examination through the electric light microscope.<sup>54</sup>

## Statistical Analyses

Data were statistically analyzed using Prism software (Graph Pad 8). Differences between groups were tested for significance using one-way analysis of variance (ANOVA), followed by the Tukey multiple comparisons test. The overall significance was indicated by the *P* value and the level of significance was set at ( $P < .05$ ) in all cases. Results were presented as means  $\pm$  standard error (S.E.) for 6 rats per group.

## Results

### Chemical Studies

#### Physicochemical characterization of GA-GaNPs

- (i) *Transmission electron microscopy*: Based on TEM images, GA-GaNPs were spherical and nearly mono-dispersed. Furthermore, size distribution suggests that the diameter of GA-GaNPs approximately ranged from 40 to 100 nm (Figure 1A: i and ii).
- (ii) *Dynamic light scattering*: Based on DLS analysis, the hydrodynamic diameter of GA-GaNPs was (91.28  $\pm$  5 nm) (Figure 1B), which is compared well with the

size estimated from the TEM images. And further, the GA-GaNPs had a negative zeta potential distribution of (-41.6 mV) (Figure 1C).

- (iii) *Fourier-transform infrared spectroscopy*: As a molecular fingerprint, the results of FTIR analysis of GA-GaNPs showed different stretches of bonds at different peaks as presented in Figure 1D. The spectrum highlighted major strong peaks and some weak peaks with a total number of 8 peaks. Strictly, a unique peak that appeared around 1020.54  $\text{cm}^{-1}$  is assigned to the Ga-OH deformation mode of a GaO(OH) moiety as reported with others,<sup>55</sup> confirming the molecular interaction between Ga(NO<sub>3</sub>)<sub>3</sub> and GA capping ligand. The assignment of bonds and their respective mode of vibration at each peak position on the FTIR spectrum are displayed in Table 2.
- (iv) *Ultraviolet-visible (UV-Vis) spectroscopy*: The UV-Vis absorption spectrum of GA-GaNPs is shown in Figure 1E, exhibiting a narrow absorption peak approximately at 270 nm assigned to surface plasmon resonance of the NPs.

### Biochemical Studies

#### In vitro study

*MTT cytotoxicity assay*. Upon incubation with HepG-2 cell line, GA-GaNPs exerted a strong cytotoxic potential in a dose-dependent manner resulting in a significant reduction of the cell proliferation (Figure 2). The IC<sub>50</sub> values were estimated from the available cytotoxicities. It is worth mentioning that GA-GaNPs displayed superior cytotoxicity than CDDP. Accordingly, it recorded a lower IC<sub>50</sub> value of (0.71  $\pm$

**Table 2.** FTIR Spectrum Assignments of GA-GaNPs.

Peak frequency ( $\text{cm}^{-1}$ )	Bond assignment (functional group)	Mode of vibration & Signal intensity (T%)	Peak frequency ( $\text{cm}^{-1}$ )	Bond assignment (functional group)	Mode of vibration & signal intensity (T%)
3453.31 $\text{cm}^{-1}$ (3500-3200)	O-H (Alcohols, phenols) <sup>57</sup>	Stretching (60.29%)	1260.74 $\text{cm}^{-1}$ (1320-1000)	C-O (Alcohols, carboxylic acids, esters & ethers) <sup>57</sup>	Stretching (78.17%)
			(1300-1150)	C-H (Alkyl halides)	Wagging (stretching) (78.17%)
2064.62 $\text{cm}^{-1}$ (~2100)	-C $\equiv$ C- (Alkynes) <sup>57</sup>	Stretching (78.81%)	1094.08 $\text{cm}^{-1}$ (1250-1020)	C-N (Aliphatic amines) <sup>57</sup>	Stretching (77.63%)
1634.42 $\text{cm}^{-1}$ (~1640)	-C=C- (Alkenes) <sup>57</sup>	Stretching (70.97%)	1020.54 $\text{cm}^{-1}$ (952-1026)	Ga-OH deformation modes of $\alpha$ -GaO(OH) <sup>55</sup>	Stretching (77.68%)
			(1320-1000)	C-O (Alcohols, carboxylic acids, esters & ethers) <sup>57</sup>	Stretching (77.68%)
1384.18 $\text{cm}^{-1}$ (1400-1290)	N-O (Nito compounds) <sup>57</sup>	Stretching (75.45%)	797.63 $\text{cm}^{-1}$ (785.05-858.35)	C-H (Phenyl ring substitution band) <sup>56</sup>	Bending (76.51%)

Abbreviations: FTIR, Fourier-transform infrared spectroscopy; GA-GaNP, gallic acid-coated gallium nanoparticles.

\*Spectrum assignments were depicted as reported by Yang *et al.*,<sup>55</sup> Ameh,<sup>56</sup> and Theivandran *et al.*<sup>57</sup>

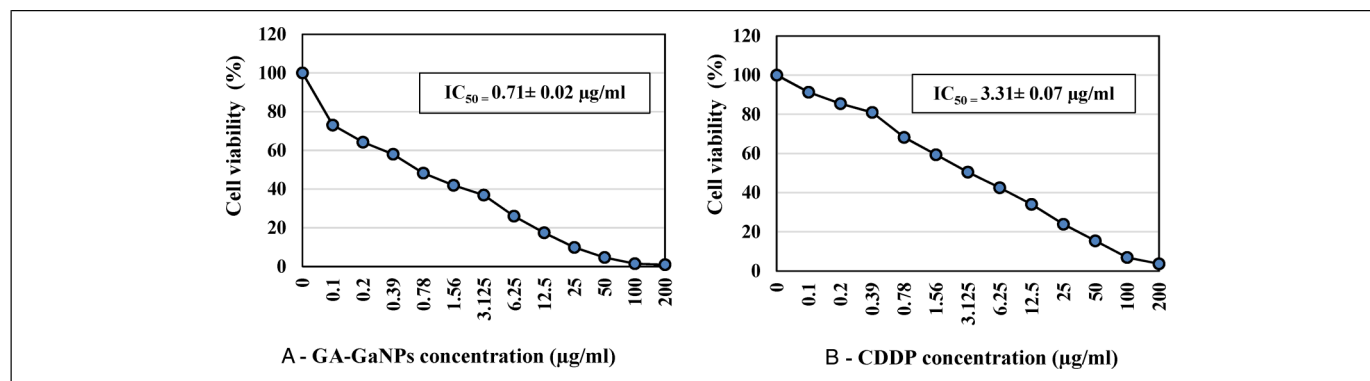


**Figure 2.** Cytotoxicity of (A) gallic acid-coated gallium nanoparticles (GA-GaNPs) and (B) CPPD against HepG-2 cell line.

**Table 3.** Alterations in C-Myc, HSP-70, and Cyt-c Relative Expression Levels Under Different Treatments.

Group parameter	C-Myc	HSP-70	Cyt-c
Control	1.01 ± 0.01 <sup>b</sup>	1.01 ± 0.007 <sup>b</sup>	1.01 ± 0.006 <sup>b</sup>
GA-GaNPs	1.017 ± 0.012 <sup>b</sup>	1.02 ± 0.02 <sup>b</sup>	1.023 ± 0.034 <sup>b</sup>
CDDP	1.003 ± 0.003 <sup>b</sup>	1.02 ± 0.02 <sup>b</sup>	1.0 ± 0.0 <sup>b</sup>
GA-GaNPs + CDDP	1.013 ± 0.018 <sup>b</sup>	1.01 ± 0.007 <sup>b</sup>	1.007 ± 0.007 <sup>b</sup>
DEN	6.9 ± 0.23 <sup>c</sup>	6.53 ± 0.203 <sup>a</sup>	0.22 ± 0.006 <sup>a</sup>
DEN + GA-GaNPs	2.075 ± 0.014 <sup>b,c</sup>	2.45 ± 0.202 <sup>b,c</sup>	0.82 ± 0.055 <sup>b,c</sup>
DEN + CDDP	1.4 ± 0.057 <sup>b</sup>	2.65 ± 0.087 <sup>b,c</sup>	0.94 ± 0.017 <sup>b</sup>
DEN + GA-GaNPs + CDDP	2.15 ± 0.14 <sup>b,c</sup>	2.08 ± 0.012 <sup>b,c</sup>	0.87 ± 0.054 <sup>b</sup>

Abbreviations: DEN, diethylnitrosamine; GA-GaNP, gallic acid-coated gallium nanoparticles.

\*Each value represents the mean ± SE of six values. Data with different superscripts are significantly different at  $P < .05$ .

<sup>a</sup>Significant versus Control group.

<sup>b</sup>Significant versus DEN group.

<sup>c</sup>Nonsignificant versus neither Control nor DEN group.

**Table 4.** Alterations in Iron Panel Levels Under Different Treatments.

Group parameter	Fe <sup>+2</sup>	TIBC	TS%
Control	19.57 ± 1.48 <sup>b</sup>	59.93 ± 5.06 <sup>b</sup>	32.75 ± 1.59 <sup>b</sup>
GA-GaNPs	21.95 ± 1.29 <sup>b</sup>	55.47 ± 1.11 <sup>b</sup>	39.64 ± 2.68 <sup>c</sup>
CDDP	20.73 ± 1.49 <sup>b</sup>	53.03 ± 4.7 <sup>b</sup>	39.5 ± 3.2 <sup>c</sup>
GA-GaNPs + CDDP	19.53 ± 0.49 <sup>b</sup>	62.95 ± 0.25 <sup>b</sup>	31.03 ± 0.48 <sup>b</sup>
DEN	43.17 ± 4.13 <sup>d</sup>	81.53 ± 2.71 <sup>d</sup>	53.25 ± 6.32 <sup>d</sup>
DEN + GA-GaNPs	18.15 ± 0.37 <sup>b</sup>	71.93 ± 1.99 <sup>c</sup>	25.3 ± 1.22 <sup>b</sup>
DEN + CDDP	19.97 ± 1.61 <sup>b</sup>	57.17 ± 4.12 <sup>b</sup>	35.48 ± 4.76 <sup>b</sup>
DEN + GA-GaNPs + CDDP	18.03 ± 1.59 <sup>b</sup>	67.77 ± 0.73 <sup>c</sup>	26.58 ± 2.17 <sup>b</sup>

Abbreviations: DEN, diethylnitrosamine; TIBC, total iron binding capacity; GA-GaNP, gallic acid-coated gallium nanoparticles.

\*Each value represents the mean ± SE of six values. Data with different superscripts are significantly different at  $P < 0.05$ .

<sup>a</sup> Significant vs Control group.

<sup>b</sup> Significant vs DEN group.

<sup>c</sup> Non-significant vs neither Control nor DEN group.

0.02 µg/mL) comparable to that of CDDP (3.31 ± 0.07 µg/mL), a result that motivated us to perform further *in vivo* preclinical investigation to test the possible efficacy of such novel nano-composite as a candidate therapy for HCC.

#### *In vivo* studies

**Acute toxicity study.** No mortality incidence was recorded after administration of elevated *i.p.* doses of GA-GaNPs up to 250 mg/kg b.wt.. By reference to Kandil *et al.*<sup>20</sup> the optimum

safe dose used for the *in vivo* treatment was calculated by dividing the highest safe dose (250 mg/kg b.wt.) by 10.

#### Evaluation of antitumor efficacy

- I. **Gene expression modulation:** Data of C-Myc, HSP-70, and Cyt-c relative expressions in liver homogenates are depicted in Table 3. DEN intoxication upregulated the mRNA expression of both C-Myc and HSP-70 genes

**Table 5.** Alterations in Biological Markers Levels Under Different Treatments.

Parameter group	AFP (ng/mL)	CASP9 (ng/mL)	VEGF (pg/mL)	GSH (mg/g)	SOD (U/g)	CAT (U/g)	MDA (nmol/g)
Control	1.03 ± 0.08 <sup>b</sup>	2.075 ± 0.01 <sup>b</sup>	37 ± 0.11 <sup>b</sup>	90.2 ± 5.65 <sup>b</sup>	5.9 ± 0.6 <sup>b</sup>	171.1 ± 5.47 <sup>b</sup>	2.38 ± 0.18 <sup>b</sup>
GA-GaNPs	0.91 ± 0.04 <sup>b</sup>	4.35 ± 0.086 <sup>b,c</sup>	35.47 ± 1.59 <sup>b</sup>	90.77 ± 4.15 <sup>b</sup>	6.07 ± 0.43 <sup>b</sup>	162.8 ± 4.6 <sup>b</sup>	2.37 ± 0.14 <sup>b</sup>
CDDP	0.89 ± 0.02 <sup>b</sup>	4.45 ± 0.086 <sup>b,c</sup>	30.27 ± 0.85 <sup>b</sup>	95.1 ± 2.34 <sup>b</sup>	6.55 ± 0.43 <sup>b</sup>	175.4 ± 1.98 <sup>b</sup>	2.55 ± 0.086 <sup>b</sup>
GA-GaNPs + CDDP	0.91 ± 0.02 <sup>b</sup>	2.07 ± 0.014 <sup>b</sup>	28.7 ± 0.63 <sup>b</sup>	80.4 ± 2.49 <sup>b</sup>	5.65 ± 0.14 <sup>b</sup>	159.5 ± 5.59 <sup>b</sup>	2.65 ± 0.086 <sup>b</sup>
DEN	3.1 ± 0.5 <sup>c</sup>	1.055 ± 0.02 <sup>c</sup>	111 ± 9.7 <sup>c</sup>	27.67 ± 2.11 <sup>c</sup>	1.45 ± 0.08 <sup>c</sup>	91.7 ± 5.54 <sup>c</sup>	72.5 ± 4.44 <sup>c</sup>
DEN + GA-GaNPs	1.88 ± 0.1 <sup>b</sup>	8.7 ± 0.11 <sup>b,c</sup>	76.8 ± 2.13 <sup>b,c</sup>	73.4 ± 0.46 <sup>b,c</sup>	4.83 ± 0.2 <sup>b</sup>	131.3 ± 8.01 <sup>b,c</sup>	18.6 ± 1.29 <sup>b,c</sup>
DEN + CDDP	1.35 ± 0.08 <sup>b</sup>	14.75 ± 0.24 <sup>b,c</sup>	67.3 ± 2.6 <sup>b,c</sup>	84.5 ± 1.04 <sup>b</sup>	5 ± 0.47 <sup>b</sup>	148.7 ± 2.05 <sup>b</sup>	18 ± 1.93 <sup>b,c</sup>
DEN + GA-GaNPs + CDDP	1.55 ± 0.14 <sup>b</sup>	8.67 ± 0.24 <sup>b,c</sup>	68.1 ± 1.6 <sup>b,c</sup>	66.9 ± 3.42 <sup>b,c</sup>	3.57 ± 0.2 <sup>b,c</sup>	115.3 ± 4.3 <sup>c</sup>	38.07 ± 1.3 <sup>b,c</sup>

Abbreviations: DEN, diethylnitrosamine; AFP, alpha-fetoprotein; VEGF, vascular endothelial growth factor; GSH, glutathione; SOD, superoxide dismutase; MDA, malondialdehyde; GA-GaNP, gallic acid-coated gallium nanoparticles.

\*Each value represents the mean ± SE of six values. Data with different superscripts are significantly different at  $P < 0.05$ .

<sup>a</sup> Significant vs Control group.

<sup>b</sup> Significant vs DEN group.

<sup>c</sup> Non-significant vs neither Control nor DEN group.

but downregulated the mRNA expression of Cyt-c gene. On contrary, treatment with GA-GaNPs, CDDP, and GA-GaNPs + CDDP of DEN-treated rats normalized liver C-Myc, HSP-70, and Cyt-c mRNA expression levels.

II. *Iron-mimicry evaluation*: Data of the monitored iron panel ( $\text{Fe}^{+2}$ , TIBC, and TS%) in liver homogenates of all studied rat groups are outlined in Table 4. The DEN-challenged group displayed significant elevations of iron ( $\text{Fe}^{+2}$ ), TIBC, and TS% values compared to their normal control counterparts. On the other side, these panel parameters have almost been ameliorated upon administrating individual GA-GaNPs and/or combined with CDDP to DEN-afflicted groups.

III. *Biological markers targeting*: Data of plasma AFP, liver CASP9, and plasma VEGF are shown in Table 5. Both plasma AFP and VEGF, as 2 major milestones in oncogenesis, have been significantly increased in the DEN-model group compared to the control one. Meanwhile, CASP9 activity has been markedly reduced upon DEN-intoxication. Administration of GA-GaNPs, CDDP, and/or GA-GaNPs + CDDP to DEN-challenged rats induced significant reductions in AFP and VEGF levels accompanied with a significant elevation in CASP9 activity exceeding normal levels upon their comparison to the DEN-model group. In addition, antioxidant enzymes (AOE) including GSH content, SOD, and CAT enzyme activities as well as MDA content in liver homogenates are shown in Table 5. It is observed that the antioxidant status in the liver of tumor-induced rats (DEN group) was significantly lower than normal, noticeable by significant depressions in GSH content, SOD, and CAT activities associated with significantly high MDA content. Individual GA-GaNPs and/or CDDP treatment, post-DEN induction, have significantly ameliorated GSH content, SOD, and CAT activities with a concomitant decline of MDA level relative to the DEN-model group.

Altogether, the aforementioned biochemical results provide a preliminary insight into the *in vivo* hierarchical action mechanism of the current nanocomplex, constituting a new initiate for alternative HCC therapeutics in the near future. Deduced molecular mechanism beyond GA-GaNPs antineoplastic action is depicted schematically in the following chart (Figure 3).

IV. *Toxicological evaluation (predicting side-effects of the current treatment)*: Results of serum liver damage and kidney damage biomarkers are recorded in Table 6. The administration of DEN to the experimental groups caused deteriorative hepatic changes presented in hampering liver functioning. Accordingly, the DEN-challenged group showed significantly elevated T.Bil levels, ALP, ALT, as well as AST activities compared to normal levels. Administration of GA-GaNPs and/or CDDP to DEN-afflicted groups ameliorated the damage by significantly reducing the abovementioned liver function indices compared to the DEN group. In tandem, shedding the light on kidney functions, DEN intoxication has been recorded to induce nephrotoxicity noticeable by significant elevations of creatinine (Cr) as well as urea levels compared to the control group. However, both of them are restored near the normal level in the treated groups.

*Histopathological findings*. Histopathologically examined liver biopsies of the different studied rat groups showed alterations in the hepatic architecture with different grades. The results are summarized in Figure 4 (H&E, 40×) and Table 7. Regarding tumor-free rat groups, liver sections of the negative control rats showed the normal histological structure of the central vein and surrounding hepatocytes in the parenchyma (Figure 4A). In a similar manner, GA-GaNPs treated livers also showed preserved hepatic architecture (Figure 4B). On contrary, livers of CDDP treated rats pointed out a fatty change in the adjacent hepatocytes of the centrilobular area

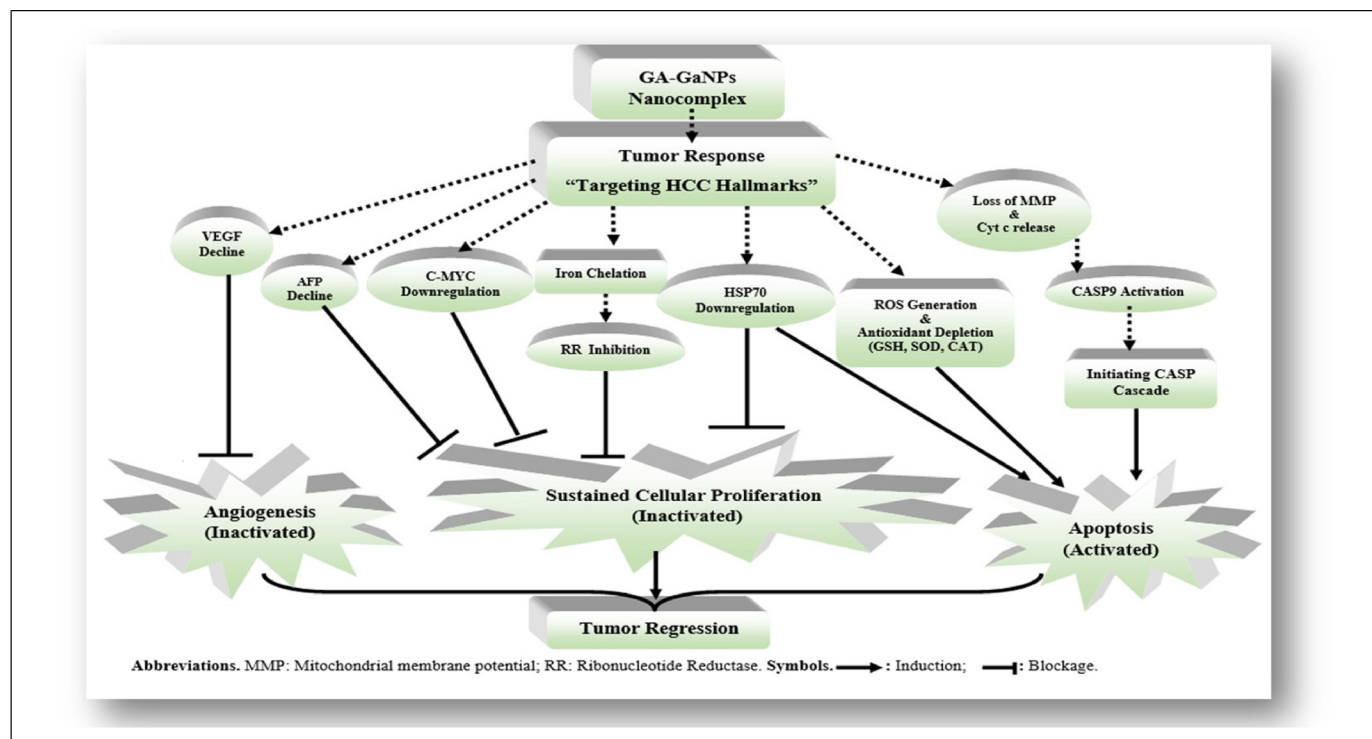


**Figure 3.** Gallic acid-coated gallium nanoparticles (GA-GaNPs) at the interface of HCC hallmarks: A schematic representation of mechanistic insights beyond GA-GaNPs antineoplastic action.

**Table 6.** Paraclinical Studies Showing Alterations in Liver and Kidney Damage Biomarkers Under Different Treatments.

Group parameter	Alb (g/dL)	T. Bil (mg/dL)	ALP (U/L)	ALT (U/mL)	AST (U/mL)	Cr (mg/dL)	Urea (mg/dL)
Control	4 ± 0.24 <sup>b</sup>	0.59 ± 0.06 <sup>c</sup>	132.5 ± 4.4 <sup>c</sup>	11 ± 0.57 <sup>c</sup>	16.33 ± 1.2 <sup>c</sup>	0.12 ± 0.002 <sup>c</sup>	34.67 ± 3.38 <sup>c</sup>
GA-GaNP	4.4 ± 0.33 <sup>c</sup>	0.64 ± 0.017 <sup>c</sup>	128.7 ± 7.1 <sup>c</sup>	12 ± 1.15 <sup>c</sup>	14 ± 0.57 <sup>c</sup>	0.12 ± 0.005 <sup>c</sup>	26 ± 0.57 <sup>c</sup>
CDDP	3.65 ± 0.26 <sup>b</sup>	0.51 ± 0.049 <sup>c</sup>	124.3 ± 1.7 <sup>c</sup>	11.67 ± 0.88 <sup>c</sup>	15.5 ± 1.44 <sup>c</sup>	0.14 ± 0.008 <sup>c</sup>	28 ± 1.73 <sup>c</sup>
GA-GaNP + CDDP	4 ± 0.4 <sup>b</sup>	0.65 ± 0.02 <sup>c</sup>	141.5 ± 2.7 <sup>c</sup>	17 ± 1.7 <sup>c</sup>	19 ± 1.16 <sup>c</sup>	0.2 ± 0.005 <sup>c</sup>	29.33 ± 2.9 <sup>c</sup>
DEN	2.77 ± 0.15 <sup>b</sup>	1.55 ± 0.14 <sup>d</sup>	351.4 ± 11.6 <sup>d</sup>	40.5 ± 2.59 <sup>d</sup>	55.5 ± 0.86 <sup>d</sup>	0.88 ± 0.05 <sup>d</sup>	75.7 ± 1.45 <sup>d</sup>
DEN + GA-GaNP	3.75 ± 0.09 <sup>b</sup>	0.75 ± 0.03 <sup>c</sup>	182.8 ± 1.5 <sup>c,d</sup>	18.5 ± 0.86 <sup>c</sup>	24 ± 1.73 <sup>c,d</sup>	0.34 ± 0.014 <sup>c,d</sup>	41 ± 1.15 <sup>c</sup>
DEN + CDDP	3.5 ± 0.12 <sup>b</sup>	0.64 ± 0.01 <sup>c</sup>	177 ± 1.9 <sup>c,d</sup>	19.5 ± 0.86 <sup>c,d</sup>	25 ± 1.15 <sup>c,d</sup>	0.26 ± 0.028 <sup>c,d</sup>	32 ± 2.51 <sup>c</sup>
DEN + GA-GaNP + CDDP	3.8 ± 0.17 <sup>b</sup>	0.71 ± 0.058 <sup>c</sup>	199.4 ± 7.03 <sup>c,d</sup>	28 ± 2.3 <sup>c,d</sup>	27 ± 1.15 <sup>c,d</sup>	0.26 ± 0.02 <sup>c,d</sup>	36.33 ± 2.33 <sup>c</sup>

Abbreviations: DEN, diethylnitrosamine; ALP, alkaline phosphatase; ALT, alanine transferase; AST, aspartate transferase; GA-GaNP, gallic acid-coated gallium nanoparticles.

\*Each value represents the mean ± SD of six values. Data with different superscripts are significantly different at P < 0.05.

<sup>a</sup> Significant vs Control group.

<sup>b</sup> Significant vs DEN group.

<sup>c</sup> Non-significant vs neither Control nor DEN group.

surrounding the dilated and congested central vein. In addition, the portal area showed fibrosis with inflammatory cell infiltration (Figure 4C). In tandem, livers of GA-GaNP + CDDP treated rats showed few inflammatory cells infiltration in the portal area with portal vein dilatation, while the surrounding hepatocytes all over the parenchyma revealed ballooning degeneration with nuclear pyknosis (Figure 4D). On the opposite side, regarding tumor-induced groups, liver sections of the DEN-model group pointed out 3 types of histopathological alterations in their hepatic architecture including: (1)

fibroblastic cell proliferation extended in between the degenerated fatty-changed hepatocytes of the parenchyma dividing it into nodules (Figure 4E), (2) inflammatory cell infiltration in the portal area and portal vein congestion, as well as, (3) hyperplasia with newly formed cystic dilated bile ducts (Figure 4F). Treatment of tumor-induced rats with GA-GaNP recorded a mild deviation from normal hepatic architecture presented in fine fibroblastic cell proliferation which divided the degenerated fatty-changed hepatocytes of the parenchyma into nodules (Figure 4G). Meanwhile, treatment of tumor-induced rats with

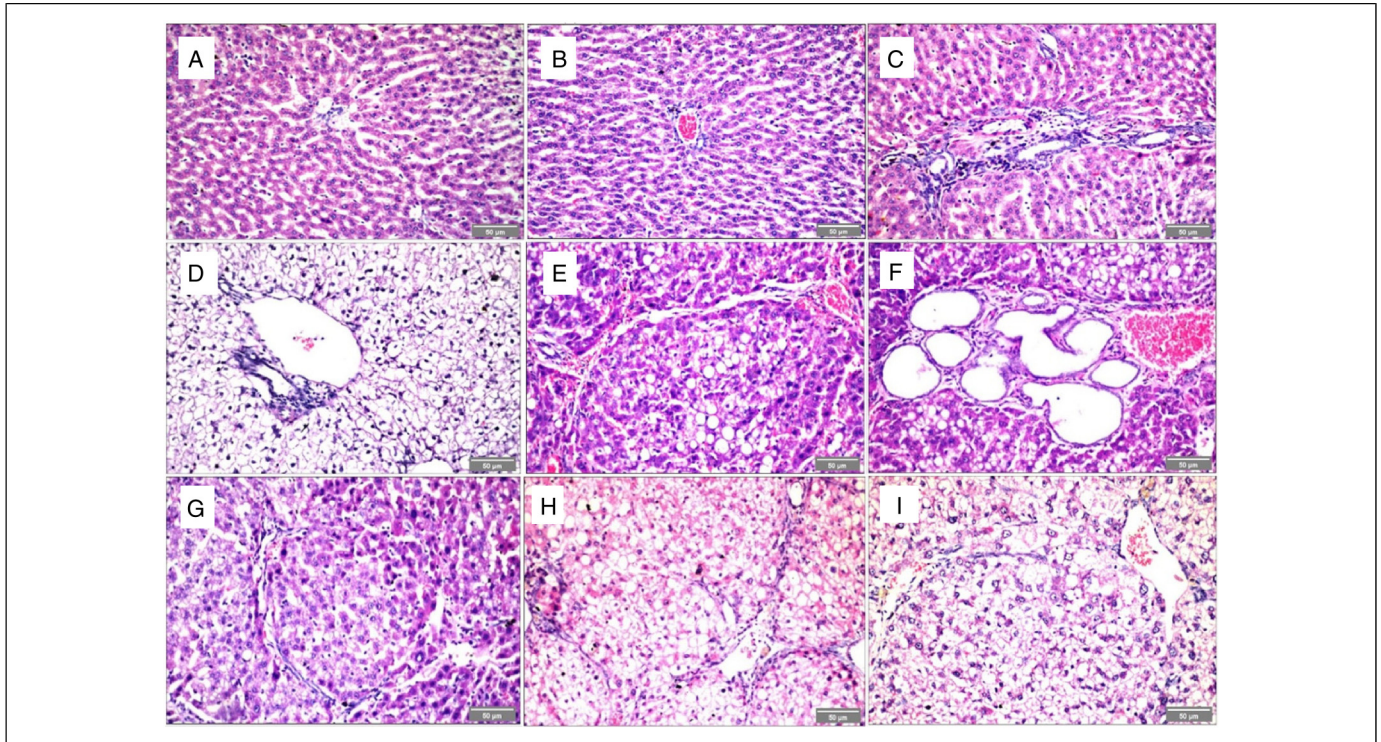


**Figure 4.** Photomicrograph of liver sections of both tumor-free and tumor-induced rat groups (hematoxylin and eosin [H&E], 40x; Scale bar = 50 μm). (A) Control; (B) gallic acid-coated gallium nanoparticles (GA-GaNP); (C) CDDP; (D) GA-GaNP + CDDP; (E and F) diethylnitrosamine (DEN) model; (G) DEN + GA-GaNP; (H) DEN + CDDP; (I) DEN + GA-GaNP + CDDP groups.

**Table 7.** Severity Grading of the Histopathological Alterations of the Hepatic Architectures Among the Different Studied Groups.

Histopathological alterations group	Control	GA-GaNP	CDDP	GA-GaNP + CDDP	DEN-model	DEN + GA-GaNP	DEN + CDDP	DEN + GA-GaNP + CDDP
a) Degenerative & fatty change in hepatocytes.	-	-	+++	+++	++	+	++	+++
b) Portal inflammatory reaction.	-	-	++	+	+	-	-	-
c) Fibrosis with nodular formation.	-	-	-	-	++	++	++	-
d) Hyperplasia & cystic dilation of bile duct.	-	-	-	-	++	-	-	-
e) Nodular eosinophilic area in parenchyma.	-	-	-	-	-	-	+	-
f) Congestion.	-	-	+	+	+	-	-	++

Abbreviations: DEN, diethylnitrosamine; GA-GaNP, gallic acid-coated gallium nanoparticles.

\*Key for histopathological alterations severity; (+++): Severe grade, (++) : Moderate grade, (+): Mild grade, and (-): Nil.

CDDP recorded less improvement where livers of this group showed fibroblastic cell proliferation dividing the ballooning-degenerated hepatocytes with pyknotic nuclei into nodules as recorded in (Figure 4H). Similarly, liver sections of DEN + GA-GaNP + CDDP treated rats showed central vein dilatation with ballooning degeneration of the hepatocytes in diffusing manner all over the parenchyma (Figure 4I).

Finally, severity grading of the histopathological alterations of the hepatic tissue architectures was also compared among the different studied rat groups (Table 7). It is worth mentioning that individual GA-GaNP treatment exhibited a superior improvement of the hepatic architecture alterations evoked over the course of chemical hepatocarcinogenesis.

## Discussion

Nowadays, understanding tumor biology and the core hallmarks of cancer have been accompanied by the development of advanced specific targeted therapies.<sup>58</sup> Nanoscale drug delivery systems have emerged as prominent methods to improve the pharmacological and therapeutic effects of many natural and synthetic drugs.<sup>59</sup> Fascinatingly, phytofabricated NPs (occasionally termed as nano-antioxidants) have been considered excellent tumor-targeting vehicles.<sup>60</sup> In this connection, such trial was projected to formulate a novel Ga-based nanocomplex under a direct molecular reduction mechanism using the non-toxic and eco-friendly phytochemical GA, as a strong reducing and stabilizing agent. This biomimetic process completely complied with the principles of green chemistry, as it used water as a benign solvent over the course of the preparation and storage of GA-GaNPs.

Former studies have evaluated the antineoplastic efficacy of some biogenic Ga-based NPs. In this connection, Kandil *et al.*<sup>20</sup> and Moawed *et al.*<sup>18</sup> have biosynthesized GaNPs using *Lactobacillus helveticus* bacterial strain and reported its therapeutic efficacy against both solid Ehrlich carcinoma and DEN-induced HCC in animal models. In tandem, Moustafa *et al.*<sup>25</sup> have also synthesized another form of biogenic Ga-based NPs using *Bacillus licheniformis* bacterial strain and reported its efficacy against brain metastasis arising from HCC. The later Ga-based NPs exert potent anticancer activity due to the reduction of Ga<sup>+2</sup> to GaO by bacterial metabolites emerging a stable NPs structure. Over and above, a most up-to-date study made by our team reported a fine antineoplastic efficacy of a biogenic Ga-based nanocomplex, coated by ellagic acid (EA), upon mammary gland-induced tumors.<sup>61</sup> Nevertheless, the currently phytofabricated Ga-based nanocomplex surpasses the later Ga-based NPs and/or complexes owing to the presence of GA coating ligand in the nanocomplex. Gallic acid phytochemical confers valuable advantages to the currently developed GA-GaNPs including: (1) enhanced antineoplastic efficacy emerging from synergistic anticancer actions of both GA and GaNPs components assembled in one compound, as well as (2) reduced toxicity owing to both antioxidant<sup>29</sup> and selective apoptosis<sup>29</sup> properties of GA. Consequently, GA has been strictly decided to act as a selective targeting ligand in the current Ga-based nanocomplex, which holds the novelty of the existing study. In this connection, it is worth mentioning that the rationale of choice of both Ga and GA to prepare the current nanocomplex is owed to their closely related anticancer mechanistic insights and multiple common oncotargets including; iron chelation,<sup>20,29,62</sup> RR inhibition,<sup>62,63</sup> ROS production,<sup>20,29,62,63</sup> GSH depletion,<sup>20,62,63</sup> loss of mitochondrial membrane potential and Cyt c release,<sup>62,63</sup> CASP9 activation,<sup>29,62,63</sup> and VEGF inhibition.<sup>25,63</sup> This in turn allowed for potentiating the synergistic anticancer action exerted by the novel GA-GaNPs nanoassembly. Over and above, the evidence that Ga compounds can tackle MDR in cancer cells<sup>24</sup> inspired us to pick Ga as a unique metal core of the current nanocomplex.

To establish its fine nanostructure, the biosynthesized GA-GaNPs was characterized *via* a panel of physicochemical analyses such as TEM, DLS, FT-IR, and UV-Vis spectroscopy. Particle size is an important property, which may influence the biological activity of NPs and has been suggested as a key factor through the interaction with charged surfaces. Current TEM images revealed NPs of diameter size ranging from 40 to 100 nm. Nanoparticles less than 100 nm are useful for biological applications. Eisenberg and coworkers<sup>64</sup> found that Ga is sensitive to ultraviolet radiation below 365 nm wavelengths. Moreover, in line with Kandil *et al.*<sup>20</sup> UV/VIS shows that the absorption spectra of GA-GaNPs were scanned at 270 nm, a finding that confirms the preservation of GaNPs in the current nanocomplex. Else more, FTIR enables the in-situ analysis of interfaces to investigate the surface adsorption of functional groups on NPs, and hence it can be used to identify the possible biomolecules responsible for capping and efficient stabilization of the synthesized metal NPs.<sup>65</sup> The FTIR spectrum of GA-GaNPs confirmed the molecular interaction between Ga(NO<sub>3</sub>)<sub>3</sub> and GA exhibiting 8 vibrational peaks (bands). Strictly, a unique peak that appeared around 1020.54 cm<sup>-1</sup> is assigned to the Ga-OH deformation mode of a GaO(OH) moiety as reported with others.<sup>55</sup> Such result can be taken as evidence for the interaction of Ga with GA, that the hydroxyl group (-OH) of GA polyphenol acts as a capping agent in controlling GaNPs size and stability. Based on DLS analysis, the hydrodynamic diameter of GA-GaNPs is compared well with the size estimated from TEM images. Last but not least, the zeta (Z) potential was measured to check the stability of the MNPs.<sup>66</sup> The more negative Z potential measure (-41.6 mV) ensures the high stability of this nanoformulation.

The *in vitro* biological evaluation of both GA-GaNPs and CDDP in a HepG-2 cancer cell line established their potential cytotoxicity. These results are in harmony with early studies that observed the *in vitro* cytotoxicities of GA,<sup>67</sup> Ga,<sup>18</sup> and CDDP<sup>68</sup> against hepatic cancer lines. It is worth mentioning that the novel GA-GaNPs displayed a superior *in vitro* cytotoxicity, as it recorded a lower IC<sub>50</sub> value comparable to that of CDDP. These results may suggest that the reaction of Ga(NO<sub>3</sub>)<sub>3</sub> with GA, at the nanoscale, resulted in super-additive cytotoxic effects towards HCC cells. On the plus side, results of the present *in vivo* study roughly postulate concerted mechanistic insights of the novel GA-GaNPs, as an alternative treatment driven by tumor biology. In this connection, various biomarkers of different molecular pathways have been simultaneously tracked, aiming at targeting key hallmarks of cancer. Three HCC hallmarks have been the main focus of the current nano-drug development which are; (1) tumorigenic potential and sustained cellular proliferation, (2) apoptosis evasion, and (3) angiogenesis induction.

Regarding tumorigenic potential, AFP is a promising marker for HCC and treatment evaluation. Accordingly, the elevation of serum AFP is indicative of the proliferation of liver progenitor cells as a response to chronic liver injury or HCC development.<sup>69</sup> In line with previous studies of Moustafa *et al.*<sup>25</sup> and Mohamed *et al.*<sup>69</sup> the current study provoked significant

elevation in AFP level in the DEN-model group compared to the normal control which might be due to DEN intoxication causing necrosis of the hepatocytes. Furthermore, such observed AFP elevation indicated the carcinogenic effect of DEN and induction of HCC. The possible explanations for the reinitiation of AFP synthesis by neoplastic hepatocytes are either increased transcription of AFP gene or posttranslational modification affecting AFP production.<sup>18</sup> Consistent with the results of Moustafa *et al.*<sup>25</sup> the present work revealed that GA-GaNPs treatment significantly dampened AFP level relative to the DEN challenged group, suggesting that GA-GaNPs might delay the process of hepatocarcinogenesis. Else more, upon potentiating the antitumorogenic efficacy of GA-GaNPs, free GA treatment of HCC-induced rats was reported to yield a remarkable reduction in serum AFP relative to the untreated HCC-afflicted counterparts.<sup>70</sup> The proposed mechanism by which GA could recover AFP serum level may stem from the suppression of COX-2 gene expression, which is known to modulate the transcription of AFP.<sup>33</sup> Collectively, as AFP is indicative for HCC, the reduction of AFP suggested the inhibition in HCC development which is further supported by the improvement of liver functions of DEN + GA-GaNPs treated rats compared to their DEN counterparts (illustrated later). On the other hand, our results are also concomitant with Mohamed *et al.*<sup>69</sup> who reported that CDDP treatment of intoxicated rats showed a significant decrease in AFP level relative to their DEN counterparts. This may be attributed to the anticancer effect of CDDP.

Li and coworkers<sup>71</sup> published that AFP stimulated the expression of some oncogenes in human HCC. Since the discovery of several important mutations that contribute to carcinogenesis (eg, c-Myc and cyclin D1 proteins), these oncogenes have been extensively used as promising targets for the development of more selective drugs to tackle cancer.<sup>72</sup> In this context, the relative expressions of some oncogenic markers have been currently quantified. The MYC proto-oncogene is a hallmark molecular feature of both the initiation and maintenance of tumorigenesis, which mainly regulates cell growth, cell cycle, metabolism, and survival. It has been implicated in the pathogenesis of most types of human tumors.<sup>73</sup> The overexpression of c-Myc has been frequently observed in the early stages of human HCC and some studies depict a strong correlation between c-Myc activation and malignant conversion of preneoplastic liver nodules into cancerous cells.<sup>5</sup> In the present study, the relative c-Myc expression has been significantly upregulated in the DEN-model group, a result that coincides with that of Ji *et al.*<sup>74</sup> who reported significant overexpression of c-Myc protein and mRNA in HCC tissues, thus promoting cell division and proliferation. In stark contrast, significant down-regulation of c-Myc relative expressions has been currently reported upon GA-GaNPs and/or CDDP treatments of tumor-induced groups, which is closely associated with growth suppression, cell cycle arrest, and loss of the neoplastic properties. Consistent with the aforementioned results, Yang & Chitambar,<sup>75</sup> reported a significant down-regulation of c-Myc differential expression upon incubation of

CCRF-CEM with Ga(NO<sub>3</sub>)<sub>3</sub>. Concurrently, Choi *et al.*<sup>76</sup> revealed that GA inhibited NF-κB-evoked expressions of cell survival genes, such as c-Myc and cyclin D1. This biochemical evidence could strictly explain the significantly dampened overexpression of c-Myc oncogene recorded in the DEN + GA-GaNPs group, highlighting the synergistic action of Ga(NO<sub>3</sub>)<sub>3</sub> and GA in growth suppression. On the plus side, in light of our results, a previous study demonstrated that c-Myc downregulation increases cellular susceptibility to CDDP in melanoma cells.<sup>77</sup> However, other studies have evoked that tumor cells surviving *in vivo* CDDP chemotherapy display c-Myc overexpression.<sup>78</sup> Mechanistically, this could be explained by provoking a DNA damage-resistance phenotype upon CDDP exposure.<sup>79</sup> Such finding gives preference to GA-GaNPs as a new initiate for HCC therapy, thus avoiding CDDP-resistant phenotype.

Targeting HSPs has emerged as a promising tempting approach to improve anticancer therapy.<sup>80</sup> The molecular chaperone HSP70 is an important mediator of HCC development by promoting tumor-initiating cells to escape self-limiting responses that restrain cell proliferation and survival.<sup>81</sup> Tumorigenic potential of tumor cells is tightly linked to the HSP70 expression.<sup>80</sup> In light of our results, the DEN-model group experienced overexpression of HSP70 relative to the negative control. Such a result could be appreciated by Halasi *et al.*<sup>82</sup> who have reported that HSP70 is overexpressed and considered to be oncogenic in different types of cancer. On the opposite side, current treatments with either GA-GaNPs and/or CDDP post-DEN induction have resulted in significant down-regulation of HSP70 expression, which selectively sensitizes malignant cells to these therapeutic agents. In line with this observation, Goloudina *et al.*<sup>83</sup> argued that the interventional anticancer approaches reducing the expression of HSP70 offer novel ways to eliminate such cancers. Furthermore, the current setting postulated that the observed downregulation of HSP70 in the DEN + GA-GaNPs group could be attributed to the GA capping portion of the nanocomplex. This presumption corresponds well with Ahmed *et al.*<sup>70</sup> who elucidated that GA administration in HCC-induced rats significantly blunted serum HSP70 level, due to the ability of GA to attenuate the expression of HSP gene.<sup>84</sup> Similarly, Sheng *et al.*<sup>85</sup> indicated that downregulating HSP70 expression enhanced the sensitivity to CDDP. Nonetheless, GA-GaNPs treatment, alone and/or combined with CDDP, displayed a superior efficacy than the individual CDDP in dampening the elevated HSP70 expression in the DEN-afflicted rats.

Over and above, altered iron metabolism is a key hallmark of cancer. During the past few years, our understanding of the genetic association and molecular mechanisms between iron and tumorigenesis has expanded enormously. The liver is the most frequently affected organ by iron overload because iron is mainly stored in hepatocytes.<sup>86</sup> Various iron-driven mechanisms have been described to induce HCC, or cancer in general. The most important of these is the generation of ROS and the resulting oxidative stress.<sup>87</sup> In this context,

patients with HCC generally contain elevated iron in their livers, indicating the critical role of iron in the stimulation of carcinogenesis.<sup>87</sup> Parallely, significantly elevated liver iron in the current DEN-intoxicated group could be appreciated by early studies of Skrajnowska *et al.*<sup>88</sup> who have reported that the neoplastic process in the organism significantly decreases iron concentration in the serum, probably by directing iron to the developing tumor. Indeed, as the cancer cells undergo massive cell division, a need for a high amount of iron for their development occurs.<sup>89</sup> On the opposite side, due to the limited understanding of the role of iron in liver cancer and the dysfunctional regulation of iron, it offers new challenges to unravel liver tumor pathogenesis and to develop new possible attractive therapeutic strategies based on iron deprivation.<sup>87</sup> This could be very probable by depleting intracellular iron stores in malignant tissues, either with the use of iron chelating agents or mimicking endogenous regulation mechanisms.<sup>90</sup> Because in this way the proliferation of tumors is limited.<sup>91</sup> Accordingly, the unique antineoplastic mechanism of Ga action that involves its ability to target and disrupt tumor cell iron homeostasis sets it apart from other chemotherapeutic drugs.<sup>62</sup> Several studies have suggested that Ga acts as an iron mimetic that can perturb cell proliferation by interposing itself into iron-dependent processes thus causing cellular iron deprivation.<sup>92</sup> In coherence with our results, Moawed *et al.*<sup>18</sup> and Kandil *et al.*<sup>20</sup> reported that treatment of tumor-bearing animal models with GaNPs significantly lowered iron levels relative to the tumor model groups. Such changes may correlate with the therapeutic effects of Ga as tumor response. Concurrently, a further effect could be attributed to the GA coat of GA-GaNPs. Accordingly, Wu *et al.*<sup>93</sup> reported that liver iron content is reduced in the soybean lecithin-gallic acid complex (SL-GAC) treated mice groups owing to the iron-chelating and antioxidant properties of the hydroxyl group in the SL-GAC (-OH group of GA), and further possibly *via* the downregulation of TfR1. These findings could in turn explain the consolidating power of the novel GA-GaNPs in depleting hepatocellular iron stores, creating an unfavorable atmosphere for the proliferation of cancer cells. The latter finding represents a novelty aspect of the present combination targeting nanotechnology. In this context, the enhanced ability of Ga-GANPs to disrupt critical iron-dependent processes in malignant cells distinguishes it from other chemotherapy-based NPs, being effective against MDR and tumor recurrence.<sup>10,62</sup> Else more, it is worth mentioning that current CDDP treatment of DEN-afflicted rats also dampened hepatic iron content relative to the DEN-model group. Finding as such might go back to the antiproliferative effect exerted by CDDP. Nonetheless, iron homeostasis (as a primary mechanistic insight of GaNPs) was much more ameliorated in the DEN + Ga-GANPs treated group than in the DEN + CDDP treated one.

Targeting the apoptotic pathway is an intriguing approach for finding new anticancer therapies, as it is nonspecific to cancer type. There are numerous mutations found in both extrinsic and intrinsic pathways in cancer, allowing the cells to evade apoptosis which is a key hallmark of cancer.

Consequently, diverse strategies and agents that target specific molecular pathways triggering apoptosis would provide a more universal cancer therapy.<sup>94</sup> The present work evoked that apoptosis induction occurs *via* pleiotropic concerted mechanisms involving Cyt-c release, CASP9 activation, ROS production, and LPO, as possible mechanistic insights through which the novel GA-GaNPs exerts its apoptotic potential.

Upon listing the apoptotic cascade players, Cyt-c is a dual-function protein that induces programmed cell death once is released from the mitochondria into the cytoplasm upon recognition and response to apoptotic stimuli by the cell.<sup>95</sup> Functionally, knockdown of Cyt-c is involved in the evasion of the apoptotic process.<sup>96</sup> In accordance, the preliminary results revealed a significant downregulation of Cyt-c relative expression in the DEN-afflicted group relative to the mock control, assuming apoptosis evasion as a hallmark of DEN-induced hepatocarcinogenesis. On contrary, GA-GaNPs and/or CDDP treatment of tumor-induced groups resulted in significant overexpression of Cyt-c being restored to near-normal level, and hence effectively suppressed the growth of cancer cells and induced cell apoptosis. Consistent with our results, Ga(NO<sub>3</sub>)<sub>3</sub> induced apoptosis in CCRF-CEM cells primarily through the mitochondrial pathway. This involves Bax activation and its translocation to the mitochondria which leads to a loss of mitochondrial membrane potential (MMP), the release of Cyt-c, and the downstream activation of executioner CASP3.<sup>97</sup> Upon further strengthening GA-GaNPs position, Tang & Cheung,<sup>98</sup> reported that GA-mediated apoptosis mainly depended on the mitochondrial pathway by promoting Cyt-c release. In tandem, Huang *et al.*<sup>31</sup> indicated that the anti-tumor effects of methyl gallate upon HCC cells occur via ROS-dependent cell death that leads to loss of MMP and Cyt-c release.<sup>99</sup> In a similar manner, Shen *et al.*<sup>100</sup> reported that CDDP treatment resulted in a significant increase in the translocation of Cyt-c from the mitochondria to the cytoplasm in HepG-2 cells.

At the top of the hierarchy of the downstream caspase cascade, the initiator CASP9 represents a pivotal signaling element governing the apoptotic commitment process.<sup>101</sup> It has emerged as a potential therapeutic target for treating cancer.<sup>102</sup> In the course of the widely held belief that apoptosis is reduced in malignancy, Cagnol *et al.*<sup>103</sup> reported that CASP-9 and -3 levels were significantly decreased in several cancers. Alongside, consistence with Chang *et al.*<sup>104</sup> current DEN-treatment resulted in a significant decrease of CASP9 concentration compared to the normal control highlighting apoptosis evasion and HCC induction. On the plus side, upregulated Cyt c in the presence of Apaf-1 activates CASP9.<sup>105</sup> In this context, marked elevations in active CASP9 concentrations have been recorded upon current administration of different treatments compared with the DEN-challenged group, suggesting the activation of the downstream CASPs and ultimately triggering apoptosis. Consensual with our literature data, Qi and coworkers<sup>106</sup> argued that Ga complexes effectively activate CASP-3, -7, and -9, promote Cyt c release, and ultimately lead to apoptosis. Concurrently, Lin *et al.*<sup>107</sup> indicated that

GA inhibited cell proliferation and promoted cell apoptosis by upregulating the ratio of cleaved CASP-9/pro-CASP-9 in HCT116 and HT29 colon cancer cells. Moreover, GA was found to induce apoptosis in the human alveolar epithelial A549 cell line through the elevation of ROS and the activation of CASP9.<sup>29</sup> Regarding CDDP, Sharma *et al.*<sup>105</sup> reported that CDDP also acts by increasing pro-apoptotic Bax concentration in the cells thereby leading to increased CASP9 activity *via* the mitochondrial pathway. However, there has been ample evidence claiming that gallates (GA) induce apoptosis selectively in fast-growing tumor cells, leaving the healthy cells intact.<sup>29</sup> This confers an additional preference to the current GA-coated GaNPs over the conventional CDDP in selective cancer targeting.

Upon complementing the apoptotic crossroads, Biroccio *et al.*<sup>77</sup> demonstrate that CASPs activation, which is essential for apoptosis induction, in the c-Myc low-expressing clones sequentially generates ROS production. In essence, there are 2 faces of ROS in cancer, pro- and anti-tumorigenic.<sup>108</sup> Accumulating evidence has demonstrated that DEN exposure has been associated with hepatocellular accumulation of ROS resulting in DNA oxidative damage, a mechanism that may further enhance DEN-induced hepatocarcinogenesis.<sup>109</sup> Similarly, the present work pointed to the likelihood that DEN-intoxication results in a heavy oxidative state revealed by serious depletion of the antioxidant grid. Recalling crossroads, it is highly plausible that the current increase of the liver function by DEN could be a secondary event following DEN-induced ROS production and LPO of hepatocyte membranes with the consequent increase in the leakage of liver enzymes.<sup>25</sup> On the opposite side, it has been suggested that oxidant generation and antioxidant depletion are common pathways through which anticancer drugs trigger apoptosis in cancer cells.<sup>24</sup> In this connection, the antitumor activity of Ga and/or GaNPs is suggested to induce their toxicity through oxidative stress by generating ROS that in turn induces apoptosis.<sup>92</sup> At the mitochondria, ROS oxidizes cardiolipin causing Cyt-c release into the cytosol, which then initiates the apoptotic cascade.<sup>110</sup> In tandem, GA phenolic antioxidant could exhibit both prooxidant as well as antioxidant characteristics displaying a dual-edge sword behavior. The prooxidant action of GA, rather than the antioxidant behavior, is responsible for its potent anticancer and selective apoptosis-inducing properties.<sup>29</sup> In that respect, Chen *et al.*<sup>111</sup> referred to the increasing evidence suggesting that apoptosis induced by GA is associated with oxidative stress derived from ROS and mitochondrial dysfunction.<sup>112</sup> Nonetheless, the current data contradicted Kandil *et al.*<sup>20</sup> who reported that GaNPs administration to tumor-bearing mice showed a marked decrease in GSH level accompanied by an increase in MDA levels relative to tumor-bearing controls. In our system, GA-GaNPs and/or GA-GaNPs + CDDP treatments significantly ameliorated the antioxidant defense grid relative to the DEN model. Such findings may be attributed to the antioxidant and free radical scavenging characteristics of the GA coat of the GA-GaNPs nano-antioxidant complex.<sup>113</sup> This observation is relevant to previous studies

highlighting the role of nano-antioxidants in the mitigation of oxidative stress-mediated toxicities. These include nano-formulations of polymer encapsulated curcumin and/or solid lipid layers of curcumin, as a naturally occurring antioxidant, have shown a robust antioxidant effect in metal-induced toxicities. In addition, plant-based silver NPs synthesized by the green approach are capable of free radical scavenging activity gaining importance in oxidative stress-mediated toxicities.<sup>59,114–116</sup> Such finding strictly discriminates the new GA-GaNPs initiate than other biosynthesized GaNPs, where it produces less oxidative damage. Over and above, the enhanced potency of GA-GaNPs in dampening MDA levels in the DEN-afflicted rats suggests their role in attenuating hepatic oxidative stress and LPO. This observation is assumably owed to the GA antioxidant coat by mitigating tissue damage caused by oxidative stress through reducing MDA levels. In stark contrast, studies made by Moustafa *et al.*<sup>25</sup> and Kandil *et al.*<sup>20</sup> have reported a significant elevation in MDA levels after GaNPs treatment relative to tumor model groups, suggesting deleterious lipid peroxidative effects to normal tissues. This finding could represent a novelty aspect of the currently developed GA-GaNPs nanocomplex over those other biogenic GaNPs in the context of cancer treatment, as lower MDA is observed and hence the oxidative damage produced is minimized. However, GA-GaNPs treatment superiorly dampened the antioxidant defense grid than CDDP relative to the mock control. This effect may be closely related to the robust prooxidant potential that emerged from GaNPs and GA assembly in one compound. Such clue could precisely confer a superior enhanced potency of GA-GaNPs than that of CPPD in triggering ROS-mediated apoptosis.

On account of HCC being a typically hypervascular tumor, anti-angiogenic treatment targeting VEGF signaling pathway remains the backbone of systemic therapy for HCC.<sup>117</sup> In harmony with the existing data, Arboatti *et al.*<sup>109</sup> evoked that DEN-intoxication significantly raised the VEGF expression pattern that is involved in triggering angiogenesis through the ERK pathway.<sup>118</sup> On the opposite side, GA-GaNPs treatment of DEN-intoxicated rats could obviously dampen VEGF levels near normal, indicating a reduction in tumor angiogenesis which further inhibited tumor growth. From where we sit, the antiangiogenic effect of GA-GaNPs could be attributed to its direct inhibitory effect on epithelial cells viability during VEGF-induced angiogenesis in endothelial cells, thereby inhibiting the development of angiogenic disorders. This finding coincides with Moustafa *et al.*<sup>25</sup> who reported that the administration of GaNPs to DEN-challenged rats significantly improves VEGF level. Strengthening the position of the novel GA-GaNPs, Subramanian *et al.*<sup>63</sup> reported that GA was found to have an antiangiogenesis property in cervical cancer and osteosarcoma cells.<sup>119</sup> Referring to CDDP, in harmony with the obtained results, Zhong *et al.*<sup>120</sup> claimed that CDDP-inhibited transcriptional activation of VEGF in a dose-dependent manner in human ovarian cancer cells. However, the results highlighted that CDDP exhibited a relatively superior angiogenic potential than that of GA-GaNPs.

A major burning issue in cancer nanomedicine is the possible toxicity of NPs induced by their systemic administration. The properties of NPs (such as shape, size, charge, surface chemistry, targeting ligands, and composition) can influence their toxicity.<sup>11,121,122</sup> Accordingly, oxidative stress is the main limitation of this study, as GA-GaNPs might lead to some sort of toxicity to both target (liver) and off-target (e.g., kidneys) organs *via* cell membrane LPO. This has been justified by toxicological evaluation of the current treatment *via* monitoring some liver & kidney damage biomarkers. Fascinatingly, it is worth mentioning that the green synthesis method of the current novel nanocomplex plays a key role in dampening its toxicity. Accordingly, in line with Moawed *et al.*<sup>18</sup> and Moustafa *et al.*<sup>25</sup> GA-GaNPs supplementation significantly restored the DEN-mediated increase of liver function indices like AST, ALT, ALP, and T.Bil toward normal levels by possibly preserving the functional integrity of the hepatocytes in those groups. Else more, concurrent with our results, Cersosimo,<sup>123</sup> showed that liver enzyme concentrations were within normal limits prior to each cycle of CDDP therapy but the AST, ALT, ALP, and LDH concentrations increased on the second day of each cycle assuming the hepatotoxic effect of CDDP. The concentrations began to decline on day 3 of each course and returned to normal by day 10 due to liver damage. This evidence could represent a plausible explanation for the dampened elevation of liver function indices in the DEN+CDDP group relative to the DEN-model one. Such clues strongly favor the synergistic role of both Ga and GA creating the effectiveness of GA-GaNPs over CDDP in maintaining the functional homeostasis of the liver, which is tightly correlated with the histopathological findings. Over and above, the aforementioned results highlight a novelty aspect of the current biogenic nanocomplex over other initiative chemotherapy-based NPs that have been modified to improve HCC therapeutics e.g., DEB-TACE, which has been associated with a higher risk for TACE-related hepatic locoregional complications.<sup>124,125</sup> Given these protective functions of both GA and Ga, this nanocomplex may also have a great potential in ameliorating DEN-induced nephrotoxicity *via* significant reduction of Cr and urea levels relative to the DEN-model group. Meanwhile, consistent with our findings Fu *et al.*<sup>126</sup> indicated that repeated low-dose CDDP treatment-induced kidney injury and atrophy with a decline in renal function. From where we sit, a plausible explanation of this finding may be owed to severe liver damage caused by CDDP, resulting in the defected urea cycle.

Gracefully written, all of the aforementioned biochemical records strictly confirmed that our DEN-induced HCC model was successful. This was well-appreciated with the histopathological picture of liver sections of the DEN-model group, mainly manifested by loss of architecture, hyperplasia, portal inflammatory reaction, fibrosis, and the presence of primary tumors. Such finding closely relates to the fact that the chronic process of inflammation is histologically related to fibrogenesis, angiogenesis, and in some cases tissue

necrosis.<sup>127</sup> Inflammatory conditions in the DEN-intoxicated group were caused by increased ROS production due to elevated intracellular iron levels, and then iron can activate NF- $\kappa$ B. On the plus side, the DEN + GA-GaNPs group displayed only mild deviation from normal liver tissue architecture indicating a remarkable improvement in the destabilized hepatic architecture, which is fully compliant with the dampened liver functioning of this group. Such improvement could be attributed to the Ga core of the current nanocomplex. A fascinating explanation could be depicted by studies of Dong *et al.*<sup>128</sup> who created Ga-doped titania nanotubes (TNTs) and further proved its efficacy in reducing inflammatory cells infiltration. Over and above, research developed nanosuspensions of gallium nitrate and alendronate (3:4) highlighted a potential synergistic effect of Ga and alendronate in immunomodulating inflammation *via* cytokines inhibition.<sup>129</sup> Thus, the cytokine profile shift after Ga treatment would help in creating an unfavorable environment for tumor growth by reducing tumor vascularization and reducing the secretion of proinflammatory cytokines into the tumor, hence blocking hyperplasia formation.<sup>127</sup> As a pro-inflammatory cytokine, NF- $\kappa$ B has a strategic position at the crossroad between oxidative stress and inflammation.<sup>130</sup> Since iron compounds are in general, pro-inflammatory, the ability of GaNPs to act as a non-functional iron mimetic may contribute to its displacement of NF- $\kappa$ B, and hence its anti-inflammatory potential.<sup>131</sup> In coherence with the Ga core, the anti-inflammatory potential of GA is attributed to NF- $\kappa$ B inhibition.<sup>93</sup> Additionally, GA has been reported to decrease the expression of inflammatory cytokines, such as interleukin 1b (IL-1b), interleukin 6 (IL-6), and IL-8. Considering this evidence, GA may also exert its antitumor effects through the modulation of inflammatory mediators.<sup>132</sup> From the histological point of view, the later facts could represent a plausible explanation for reducing inflammation in the liver architecture of the DEN + GA-GaNPs treated group. Such clues strongly favor the synergistic action of both Ga and GA in creating the effectiveness of GA-GaNPs nano-drug in maintaining the liver architecture. Meanwhile, treatment with CDDP recorded less improvement, which may be attributed to the hepatotoxic effect of CDDP *in vivo*.<sup>133</sup> Last but not least, severity grading of the histopathological alterations among the different studied groups highlighted that individual GA-GaNPs treatment showed the most preferable risk-benefit profile in struggling primary hepatocarcinogenesis, which serves as a novelty aspect of the existing study.

## Conclusion and Future Perspectives

The aforementioned results can postulate that the reaction of Ga(NO<sub>3</sub>)<sub>3</sub> with GA, following the principles of green synthesis of NPs, resulted in super-additive cytotoxic effects at the interface of primary hepatocarcinogenesis. In this context, the existing study provides a preliminary insight into a hierarchical antineoplastic action mechanism of the novel GA-GaNPs mainly *via* governing some HCC hallmarks, such as sustained

cellular proliferation, apoptosis evasion, and angiogenesis induction. This was well-appreciated with the histopathological survey of the studied groups. Collectively, the results highlighted that individual supplementation of GA-GaNPs exhibits a more preferable risk-benefit profile than that of CDDP in struggling primary hepatocarcinogenesis. Else more, it is worth mentioning that the combined supplementation of GA-GaNPs with CDDP hasn't significantly enhanced the effect shown by the individual GA-GaNPs treatment. In conclusion, such findings suggest that novel phytofabricated Ga-based nanocomplexes can be recommended for future HCC therapeutic disciplines, although human studies are still in the queue.

### Authors' Note

All the authors contributed to the data analysis, drafting, discussion of the results, and approval of the final manuscript. Animal maintenance and treatments were conducted in accordance with International Guiding Principles, as approved by Research Ethics Committee in National Center for Research and Technology (REC-NCRRT) with Sanction No. 82A/21.

### Acknowledgments

The authors thank Prof. Dr. Adel Bakeer Kholousy, Professor of Pathology, Cairo University, for his great effort in performing the histopathological survey.

### Declaration of Conflicting Interests

The author(s) declared no potential conflicts of interest with respect to the research, authorship, and/or publication of this article.

### Funding

The author(s) received no financial support for the research, authorship, and/or publication of this article.

### ORCID iD

Nihal Mostafa  <https://orcid.org/0000-0002-9180-0630>

### References

- Baboci L, Capolla S, Di Cintio F, et al. The dual role of the liver in nanomedicine as an actor in the elimination of nanostructures or a therapeutic target. *J Oncol*. 2020;2020:4638192. doi:10.1155/2020/4638192
- Llovet JM, Kelley RK, Villanueva A, et al. Hepatocellular carcinoma. *Nat Rev Dis Primers*. 2021;7(1):6. doi:10.1038/s41572-020-00240-3
- Sia D, Villanueva A, Friedman SL, Llovet JM. Liver cancer cell of origin, molecular class, and effects on patient prognosis. *Gastroenterology*. 2017;152(4):745-761. doi:10.1053/j.gastro.2016.11.048
- Golabi P, Fazel S, Otgonsuren M, Sayiner M, Locklear CT, Younossi ZM. Mortality assessment of patients with hepatocellular carcinoma according to underlying disease and treatment modalities. *Medicine (Baltimore)*. 2017;96(9):e5904. doi:10.1097/MD.0000000000005904
- Alqahtani A, Khan Z, Alloghbi A, Said Ahmed TS, Ashraf M, Hammouda DM. Hepatocellular carcinoma: molecular mechanisms and targeted therapies. *Medicina (Kaunas)*. 2019;55(9):526. doi:10.3390/medicina55090526
- Simile MM, Bagella P, Vidili G, et al. Targeted therapies in cholangiocarcinoma: emerging evidence from clinical trials. *Medicina (Kaunas)*. 2019;55(2):42. doi:10.3390/medicina55020042
- Roberts LR, Gores GJ. Hepatocellular carcinoma: molecular pathways and new therapeutic targets. *Semin Liver Dis*. 2005;25(2):212-225. doi:10.1055/s-2005-871200
- Ahmadian E, Dizaj SM, Sharifi S, et al. The potential of nanomaterials in theranostics of oral squamous cell carcinoma: recent progress. *Trends Analyt Chem*. 2019;116:167-176.
- Morovati A, Ahmadian S, Jafary H. Cytotoxic effects and apoptosis induction of cisplatin-loaded iron oxide nanoparticles modified with chitosan in human breast cancer cells. *Mol Biol Rep*. 2019;46(5):5033-5039. doi:10.1007/s11033-019-04954-w
- Sun Y, Ma W, Yang Y, et al. Cancer nanotechnology: enhancing tumor cell response to chemotherapy for hepatocellular carcinoma therapy. *Asian J Pharm Sci*. 2019;14(6):581-594. doi:10.1016/j.ajps.2019.04.005
- Chowdhury MMH, Salazar CJJ, Nurunnabi M. Recent advances in bionanomaterials for liver cancer diagnosis and treatment. *Biomater Sci*. 2021;9(14):4821-4842. doi:10.1039/d1bm00167a
- Anselmo AC, Mitragotri S. Nanoparticles in the clinic. *Bioeng Transl Med*. 2016;1(1):10-29. doi:10.1002/btm2.10003
- Ventola CL. Progress in nanomedicine: approved and investigational nanodrugs. *P T*. 2017;42(12):742-755.
- Facciorusso A. Drug-eluting beads transarterial chemoembolization for hepatocellular carcinoma: current state of the art. *World J Gastroenterol*. 2018;24(2):161-169. doi:10.3748/wjg.v24.i2.161
- Chang WC, Hsu HH, Chiu SH, et al. Transcatheter arterial chemoembolization with drug-eluting beads for the treatment of hepatocellular carcinoma: recommended selection for small-caliber (<100  $\mu$ m) beads. *J Hepatocell Carcinoma*. 2021;8:937-949. doi:10.2147/JHC.S319920
- Wei QY, He KM, Chen JL, Xu YM, Lau ATY. Phytofabrication of nanoparticles as novel drugs for anticancer applications. *Molecules*. 2019;24(23):4246. doi:10.3390/molecules24234246
- Reineck P, Lin Y, Gibson BC, Dickey MD, Greentree AD, Maksymov IS. UV Plasmonic properties of colloidal liquid-metal eutectic gallium-indium alloy nanoparticles. *Sci Rep*. 2019;9(1):5345. doi:10.1038/s41598-019-41789-8
- Moawed FS, El-Sonbaty SM, Mansour SZ. Gallium nanoparticles along with low-dose gamma radiation modulate TGF- $\beta$ /MMP-9 expression in hepatocellular carcinogenesis in rats. *Tumour Biol*. 2019;41(3):1010428319834856. doi:10.1177/1010428319834856
- Yang L. *Investigation of Novel Nanoparticles of Gallium Ferricyanide and Gallium Lawsonate as Potential Anticancer Agents, and Nanoparticles of Novel Bismuth Tetrathiotungstate as Promising CT Contrast Agent*. Kent State University; 2014.
- Kandil EI, El-Sonbaty SM, Moawed FS, Khedr OM. Anticancer redox activity of gallium nanoparticles accompanied with low dose of gamma radiation in female mice. *Tumour Biol*. 2018;40(3):1010428317749676. doi:10.1177/1010428317749676

21. Robin P, Singh K, Suntharalingam K. Gallium(iii)-polypyridyl complexes as anti-osteosarcoma stem cell agents. *Chem Commun (Camb)*. 2020;56(10):1509-1512. doi:10.1039/c9cc08962d
22. Chua MS, Bernstein LR, Li R, So SK. Gallium maltolate is a promising chemotherapeutic agent for the treatment of hepatocellular carcinoma. *Anticancer Res*. 2006;26(3A):1739-1743.
23. Chitambar CR, Antholine WE. Iron-targeting antitumor activity of gallium compounds and novel insights into triapine(®)-metal complexes. *Antioxid Redox Signal*. 2013;18(8):956-972. doi:10.1089/ars.2012.4880
24. Salem A, Noaman E, Kandil E, Badawi A, Mostafa N. Crystal structure and chemotherapeutic efficacy of the novel compound, gallium tetrachloride betaine, against breast cancer using nanotechnology. *Tumour Biol*. 2016;37(8):11025-11038. doi:10.1007/s13277-016-4969-2
25. Moustafa EM, Mohamed MA, Thabet NM. Gallium nanoparticle-mediated reduction of brain specific serine protease-4 in an experimental metastatic cancer model. *Asian Pac J Cancer Prev*. 2017;18(4):895-903. doi:10.22034/APJCP.2017.18.4.895
26. Lessa JA, Parrilha GL, Beraldo H. Gallium complexes as new promising metallodrugs candidates. *Inorganica Chim Acta*. 2012;393:53-63.
27. Halevas E, Mavroidi B, Antonoglou O, et al. Structurally characterized gallium-chrysin complexes with anticancer potential. *Dalton Trans*. 2020;49(8):2734-2746. doi:10.1039/c9dt04540f
28. Kang DY, Sp N, Jo ES, et al. The inhibitory mechanisms of tumor PD-L1 expression by natural bioactive gallic acid in non-small-cell lung cancer (NSCLC) cells. *Cancers (Basel)*. 2020;12(3):727. doi:10.3390/cancers12030727
29. Badhani B, Sharma N, Kakkar R. Gallic acid: a versatile antioxidant with promising therapeutic and industrial applications. *RSC Adv*. 2015;5(35):27540-27557.
30. Sun G, Zhang S, Xie Y, Zhang Z, Zhao W. Gallic acid as a selective anticancer agent that induces apoptosis in SMMC-7721 human hepatocellular carcinoma cells. *Oncol Lett*. 2016;11(1):150-158. doi:10.3892/ol.2015.3845
31. Huang CY, Chang YJ, Wei PL, Hung CS, Wang W. Methyl gallate, gallic acid-derived compound, inhibit cell proliferation through increasing ROS production and apoptosis in hepatocellular carcinoma cells. *PLoS One*. 2021;16(3):e0248521. doi:10.1371/journal.pone.0248521
32. Jagan S, Ramakrishnan G, Anandakumar P, Kamaraj S, Devaki T. Antiproliferative potential of gallic acid against diethylnitrosamine-induced rat hepatocellular carcinoma. *Mol Cell Biochem*. 2008;319(1-2):51-59. doi:10.1007/s11010-008-9876-4
33. Aglan HA, Ahmed HH, El-Toumy SA, Mahmoud NS. Gallic acid against hepatocellular carcinoma: an integrated scheme of the potential mechanisms of action from in vivo study. *Tumour Biol*. 2017;39(6):1010428317699127. doi:10.1177/1010428317699127
34. Arsianti A, Bahtiar A, Fadilah F, et al. Synthesis, characterization, and cytotoxicity evaluation of gallic acid nanoparticles towards breast T47D cancer cells. *Pharmacogn J*. 2020;12(2).
35. Baig B, Halim SA, Farrukh A, Greish Y, Amin A. Current status of nanomaterial-based treatment for hepatocellular carcinoma. *Biomed Pharmacother*. 2019;116:108852. doi:10.1016/j.biopha.2019.108852
36. Verma S, Singh A, Mishra A. Gallic acid: molecular rival of cancer. *Environ Toxicol Pharmacol*. 2013;35(3):473-485. doi:10.1016/j.etap.2013.02.011
37. Varela-Rodríguez L, Sánchez-Ramírez B, Hernández-Ramírez VI, et al. Effect of gallic acid and myricetin on ovarian cancer models: a possible alternative antitumoral treatment. *BMC Complement Med Ther*. 2020;20(1):110. doi:10.1186/s12906-020-02900-z
38. National Research Council (US) Committee for the Update of the Guide for the Care and Use of Laboratory Animals. *Guide for the Care and Use of Laboratory Animals*. 8th ed. National Academies Press (US); 2011. <https://pubmed.ncbi.nlm.nih.gov/21595115/#:~:text=The%20purpose%20of%20the%20Guide%20for%20the%20Care,judged%20to%20be%20scientifically%2C%20technically%2C%20and%20humanely%20appropriate.>
39. Percie du Sert N, Hurst V, Ahluwalia A, et al. The ARRIVE guidelines 2.0: updated guidelines for reporting animal research. *Br J Pharmacol*. 2020;177(16):3617-3624. doi:10.1111/bph.15193
40. Li D, Liu Z, Yuan Y, Liu Y, Niu F. Green synthesis of gallic acid-coated silver nanoparticles with high antimicrobial activity and low cytotoxicity to normal cells. *Process Biochem*. 2015;50(3):357-366.
41. Gurunathan S, Kalishwaralal K, Vaidyanathan R, et al. Biosynthesis, purification and characterization of silver nanoparticles using *Escherichia coli*. *Colloids Surf B Biointerfaces*. 2009;74(1):328-335. doi:10.1016/j.colsurfb.2009.07.048
42. van Meerloo J, Kaspers GJ, Cloos J. Cell sensitivity assays: the MTT assay. *Methods Mol Biol*. 2011;731:237-245. doi:10.1007/978-1-61779-080-5\_20
43. Darwish HA, EL-Boghdady NA. Possible involvement of oxidative stress in diethylnitrosamine-induced hepatocarcinogenesis: chemopreventive effect of curcumin. *J Food Biochem*. 2013;37(3):353-361.
44. Chen Y, Han F, Cao LH, et al. Dose-response relationship in cisplatin-treated breast cancer xenografts monitored with dynamic contrast-enhanced ultrasound. *BMC Cancer*. 2015;15(1):1-9. doi:10.1186/s12885-015-1170-8
45. Beutler E, Duron O, Kelly BM. Improved method for the determination of blood glutathione. *J Lab Clin Med*. 1963;61:882-888.
46. Nishikimi M, Appaji N, Yagi K. The occurrence of superoxide anion in the reaction of reduced phenazine methosulfate and molecular oxygen. *Biochem Biophys Res Commun*. 1972;46(2):849-854. doi:10.1016/s0006-291x(72)80218-3
47. Aebi H. [13] catalase in vitro. *Methods Enzymol*. 1984;105: 121-126.
48. Fossati P, Prencipe L, Berti G. Use of 3,5-dichloro-2-hydroxybenzenesulfonic acid/4-aminophenazone chromogenic system in direct enzymic assay of uric acid in serum and urine. *Clin Chem*. 1980;26(2):227-231.
49. Ohkawa H, Ohishi N, Yagi K. Assay for lipid peroxides in animal tissues by thiobarbituric acid reaction. *Anal Biochem*. 1979;95(2):351-358. doi:10.1016/0003-2697(79)90738-3
50. Doumas BT, Watson WA, Biggs HG. Albumin standards and the measurement of serum albumin with bromocresol green. *Clin Chim Acta*. 1971;31(1):87-96. doi:10.1016/0009-8981(71)90365-2

51. Walters MI, Gerarde HW. An ultramicromethod for the determination of conjugated and total bilirubin in serum or plasma. *Microchem J.* 1970;15(2):231-243.
52. Belfield A, Goldberg DM. Revised assay for serum phenyl phosphatase activity using 4-amino-antipyrine. *Enzyme.* 1971;12(5):561-573. doi:10.1159/000459586
53. Reitman S, Frankel S. A colorimetric method for the determination of serum glutamic oxalacetic and glutamic pyruvic transaminases. *Am J Clin Pathol.* 1957;28(1):56-63. doi:10.1093/ajcp/28.1.56
54. Bancroft JD, Gamble M, eds. *Theory and Practice of Histological Techniques.* Elsevier Health Science; 2008.
55. Yang JJ, Zhao Y, Frost RL. Infrared and infrared emission spectroscopy of gallium oxide alpha-GaO(OH) nanostructures. *Spectrochim Acta A Mol Biomol Spectrosc.* 2009;74(2):398-403. doi:10.1016/j.saa.2009.06.032
56. Ameh PO. Inhibitory action of Albizia zygia gum on mild steel corrosion in acid medium. *Afr J Pure Appl Chem.* 2014;8(2):37-46.
57. Theivandran G, Ibrahim SM, Murugan M. Fourier Transform infrared (Ft-IR) spectroscopic analysis of spirulina fusiformis. *J Med Plants Stud.* 2015;3(4):30-32.
58. Al-Bedeary S, Getta HA, Al-Sharafi D. The hallmarks of cancer and their therapeutic targeting in current use and clinical trials. *Iraqi J Hematol.* 2020;9(1):1. Published 2020 Jan 1.
59. Eftekhari A, Dizaj SM, Chodari L, et al. The promising future of nano-antioxidant therapy against environmental pollutants induced-toxicities. *Biomed Pharmacother.* 2018;103:1018-1027. doi:10.1016/j.biopha.2018.04.126
60. Baranwal A, Mahato K, Srivastava A, Maurya PK, Chandra P. Phytofabricated metallic nanoparticles and their clinical applications. *RSC Adv.* 2016;6(107):105996-106010.
61. El-sonbaty SM, Moawed FSM, Kandil EI, Tamamm AM. Antitumor and antibacterial efficacy of gallium nanoparticles coated by ellagic acid. *Dose Response.* 2022; 20(1):1-15. doi:10.1177/15593258211068998
62. Chitambar CR, Al-Gizawiy MM, Alhajala HS, et al. Gallium maltolate disrupts tumor iron metabolism and retards the growth of glioblastoma by inhibiting mitochondrial function and ribonucleotide reductase. *Mol Cancer Ther.* 2018;17(6):1240-1250. doi:10.1158/1535-7163.MCT-17-1009
63. Subramanian AP, John AA, Vellayappan MV, et al. Gallic acid: prospects and molecular mechanisms of its anticancer activity. *RSC Adv.* 2015;5(45):35608-35621.
64. Eisenberg I, Alpern H, Gutkin V, Yochelis S, Paltiel Y. Dual mode UV/visible-IR gallium-nitride light detector. *Sens Actuator A Phys.* 2015;233:26-31.
65. Mudunkotuwa IA, Minshid AA, Grassian VH. ATR-FTIR spectroscopy as a tool to probe surface adsorption on nanoparticles at the liquid-solid interface in environmentally and biologically relevant media. *Analyst.* 2014;139(5):870-881. doi:10.1039/c3an01684f
66. Irvani S. Green synthesis of metal nanoparticles using plants. *Green Chem.* 2011;13(10):2638-2650.
67. Hassani A, Azarian MMS, Ibrahim WN, Hussain SA. Preparation, characterization and therapeutic properties of gum arabic-stabilized gallic acid nanoparticles. *Sci Rep.* 2020;10(1):17808. doi:10.1038/s41598-020-71175-8
68. Li Y, Zhang X, Yang X, et al. Differential effects of ginkgol C17:1 on cisplatin-induced cytotoxicity: protecting human normal L02 hepatocytes versus sensitizing human hepatoma HepG2 cells. *Oncol Lett.* 2019;17(3):3181-3190. doi:10.3892/ol.2019.9974
69. Mohamed NZ, Aly HF, Moneim El-Mezayen HA, El-Salamony HE. Effect of co-administration of Bee honey and some chemotherapeutic drugs on dissemination of hepatocellular carcinoma in rats. *Toxicol Rep.* 2019;6:875-888. doi:10.1016/j.toxrep.2019.08.007
70. Ahmed HH, Galal AF, Shalby AB, Abd-Rabou AA, Mehaya FM. Improving anti-cancer potentiality and bioavailability of gallic acid by designing polymeric nanocomposite formulation. *Asian Pac J Cancer Prev.* 2018;19(11):3137-3146. doi:10.31557/APJCP.2018.19.11.3137
71. Li MS, Li PF, Chen Q, Du GG, Li G. Alpha-fetoprotein stimulated the expression of some oncogenes in human hepatocellular carcinoma Bel 7402 cells. *World J Gastroenterol.* 2004;10(6):819-824. doi:10.3748/wjg.v10.i6.819
72. Roma-Rodrigues C, Mendes R, Baptista PV, Fernandes AR. Targeting tumor microenvironment for cancer therapy. *Int J Mol Sci.* 2019;20(4):840. doi:10.3390/ijms20040840
73. Elbadawy M, Usui T, Yamawaki H, Sasaki K. Emerging roles of C-Myc in cancer stem cell-related signaling and resistance to cancer chemotherapy: a potential therapeutic target against colorectal cancer. *Int J Mol Sci.* 2019;20(9):2340. doi:10.3390/ijms20092340
74. Ji F, Zhang ZH, Zhang Y, et al. Low expression of c-Myc protein predicts poor outcomes in patients with hepatocellular carcinoma after resection. *BMC Cancer.* 2018;18(1):460. doi:10.1186/s12885-018-4379-5
75. Yang M, Chitambar CR. Role of oxidative stress in the induction of metallothionein-2A and heme oxygenase-1 gene expression by the antineoplastic agent gallium nitrate in human lymphoma cells. *Free Radic Biol Med.* 2008;45(6):763-772. doi:10.1016/j.freeradbiomed.2008.05.031
76. Choi KC, Lee YH, Jung MG, et al. Gallic acid suppresses lipopolysaccharide-induced nuclear factor-kappaB signaling by preventing RelA acetylation in A549 lung cancer cells. *Mol Cancer Res.* 2009;7(12):2011-2021. doi:10.1158/1541-7786.MCR-09-0239
77. Biroccio A, Benassi B, Amodei S, Gabellini C, Del Bufalo D, Zupi G. c-Myc down-regulation increases susceptibility to cisplatin through reactive oxygen species-mediated apoptosis in M14 human melanoma cells. *Mol Pharmacol.* 2001;60(1):174-182. doi:10.1124/mol.60.1.174
78. Walker TL, White JD, Esdale WJ, Burton MA, DeCruz EE. Tumour cells surviving in vivo cisplatin chemotherapy display elevated c-myc expression. *Br J Cancer.* 1996;73(5):610-614. doi:10.1038/bjc.1996.105
79. Robinson AM, Rathore R, Redlich NJ, et al. Cisplatin exposure causes c-Myc-dependent resistance to CDK4/6 inhibition in HPV-negative head and neck squamous cell carcinoma. *Cell Death Dis.* 2019;10(11):867. doi:10.1038/s41419-019-2098-8

80. Albakova Z, Armeev GA, Kanevskiy LM, Kovalenko EI, Sapozhnikov AM. HSP70 multi-functionality in cancer. *Cells*. 2020;9(3):587. doi:10.3390/cells9030587
81. Cho W, Jin X, Pang J, Wang Y, Mivechi NF, Moskophidis D. The molecular chaperone heat shock protein 70 controls liver cancer initiation and progression by regulating adaptive DNA damage and mitogen-activated protein kinase/extracellular signal-regulated kinase signaling pathways. *Mol Cell Biol*. 2019;39(9):e00391-18. doi:10.1128/MCB.00391-18
82. Halasi M, Váraljai R, Benevolenskaya E, Gartel AL. A novel function of molecular chaperone HSP70: suppression of oncogenic foxm1 after proteotoxic stress. *J Biol Chem*. 2016;291(1):142-148. doi:10.1074/jbc.M115.678227
83. Goloudina AR, Demidov ON, Garrido C. Inhibition of HSP70: a challenging anti-cancer strategy. *Cancer Lett*. 2012;325(2):117-124. doi:10.1016/j.canlet.2012.06.003
84. Sobeh M, ElHawary E, Peixoto H, et al. Identification of phenolic secondary metabolites from *Schotia brachypetala* sond. (fabaceae) and demonstration of their antioxidant activities in *Caenorhabditis elegans*. *PeerJ*. 2016;4:e2404. doi:10.7717/peerj.2404
85. Sheng L, Tang T, Liu Y, et al. Inducible HSP70 antagonizes cisplatin-induced cell apoptosis through inhibition of the MAPK signaling pathway in HGC-27 cells. *Int J Mol Med*. 2018;42(4):2089-2097. doi:10.3892/ijmm.2018.3789
86. Li Y, Huang X, Wang J, Huang R, Wan D. Regulation of iron homeostasis and related diseases. *Mediators Inflamm*. 2020;2020:6062094. doi:10.1155/2020/6062094
87. Paganoni R, Lechel A, Vujic Spasic M. Iron at the interface of hepatocellular carcinoma. *Int J Mol Sci*. 2021;22(8):4097. doi:10.3390/ijms22084097
88. Skrajnawska D, Bobrowska B, Tokarz A, Kuras M. The effect of copper and resveratrol on hair mineral concentrations in rats with DMBA-induced mammary cancer. *Bromat Chem Toksykol*. 2012;3:580-585.
89. Gurzau ES, Neagu C, Gurzau AE. Essential metals--case study on iron. *Ecotoxicol Environ Saf*. 2003;56(1):190-200. doi:10.1016/s0147-6513(03)00062-9
90. Brown RAM, Richardson KL, Kabir TD, Trinder D, Ganss R, Leedman PJ. Altered iron metabolism and impact in cancer biology, metastasis, and immunology. *Front Oncol*. 2020;10:476. doi:10.3389/fonc.2020.00476
91. Bobrowska-Korczak B, Skrajnawska D, Tokarz A. The effect of dietary zinc--and polyphenols intake on DMBA-induced mammary tumorigenesis in rats. *J Biomed Sci*. 2012;19(1):43. doi:10.1186/1423-0127-19-43
92. Chitambar CR. Gallium-containing anticancer compounds. *Future Med Chem*. 2012;4(10):1257-1272. doi:10.4155/fmc.12.69
93. Wu X, Wang Y, Jia R, Fang F, Liu Y, Cui W. Computational and biological investigation of the soybean lecithin-gallic acid complex for ameliorating alcoholic liver disease in mice with iron overload. *Food Funct*. 2019;10(8):5203-5214. doi:10.1039/c9fo01022j
94. Pfeffer CM, Singh ATK. Apoptosis: a target for anticancer therapy. *Int J Mol Sci*. 2018;19(2):448. doi:10.3390/ijms19020448
95. Figueroa CM, Suárez BN, Molina AM, Fernández JC, Torres Z, Griebenow K. Smart release nano-formulation of cytochrome C and hyaluronic acid induces apoptosis in cancer cells. *J Nanomed Nanotechnol*. 2017;8(1):427. doi:10.4172/2157-7439.1000427
96. Liu Z, Zhao X, Zhang L, Pei B. Cytochrome C inhibits tumor growth and predicts favorable prognosis in clear cell renal cell carcinoma. *Oncol Lett*. 2019;18(6):6026-6032. doi:10.3892/ol.2019.10989
97. Chitambar CR, Wereley JP, Matsuyama S. Gallium-induced cell death in lymphoma: role of transferrin receptor cycling, involvement of Bax and the mitochondria, and effects of proteasome inhibition. *Mol Cancer Ther*. 2006;5(11):2834-2843. doi:10.1158/1535-7163.MCT-06-0285
98. Tang HM, Cheung PCK. Gallic acid triggers iron-dependent cell death with apoptotic, ferroptotic, and necroptotic features. *Toxins (Basel)*. 2019;11(9):492. doi:10.3390/toxins11090492
99. Marchi S, Giorgi C, Suski JM, et al. Mitochondria-ros crosstalk in the control of cell death and aging. *J Signal Transduct*. 2012;2012:329635. doi:10.1155/2012/329635
100. Shen X, Gao X, Li H, Gu Y, Wang J. TIMP-3 Increases the chemosensitivity of laryngeal carcinoma to cisplatin via facilitating mitochondria-dependent apoptosis. *Oncol Res*. 2018;27(1):73-80. doi:10.3727/096504018X15201099883047
101. Li P, Zhou L, Zhao T, et al. Caspase-9: structure, mechanisms and clinical application. *Oncotarget*. 2017;8(14):23996-24008. doi:10.18632/oncotarget.15098
102. Kim B, Srivastava SK, Kim SH. Caspase-9 as a therapeutic target for treating cancer. *Expert Opin Ther Targets*. 2015;19(1):113-127. doi:10.1517/14728222.2014.961425
103. Cagnol S, Mansour A, Van Obberghen-Schilling E, Chambard JC. Raf-1 activation prevents caspase 9 processing downstream of apoptosome formation. *J Signal Transduct*. 2011;2011:834948. doi:10.1155/2011/834948
104. Chang W, He W, Li PP, et al. Protective effects of celastrol on diethylnitrosamine-induced hepatocellular carcinoma in rats and its mechanisms. *Eur J Pharmacol*. 2016;784:173-180. doi:10.1016/j.ejphar.2016.04.045
105. Sharma H, Sen S, Singh N. Molecular pathways in the chemosensitization of cisplatin by quercetin in human head and neck cancer. *Cancer Biol Ther*. 2005;4(9):949-955. doi:10.4161/cbt.4.9.1908
106. Qi J, Yao Q, Qian K, Tian L, Cheng Z, Wang Y. Gallium(III) complexes of  $\alpha$ -N-heterocyclic piperidylthiosemicarbazones: synthesis, structure-activity relationship, cellular uptake and activation of caspases-3/7/9. *J Inorg Biochem*. 2018;186:42-50. doi:10.1016/j.jinorgbio.2018.05.005
107. Lin X, Wang G, Liu P, et al. Gallic acid suppresses colon cancer proliferation by inhibiting SRC and EGFR phosphorylation. *Exp Ther Med*. 2021;21(6):638. doi:10.3892/etm.2021.10070
108. Reczek CR, Chandel NS. The two faces of reactive oxygen species in cancer. *Annu Rev Cancer Biol*. 2017;1:79-98.
109. Arboatti AS, Lambertucci F, Sedlmeier MG, et al. Diethylnitrosamine increases proliferation in early stages of hepatic carcinogenesis in insulin-treated type 1 diabetic mice. *Biomed Res Int*. 2018;2018:9472939. doi:10.1155/2018/9472939

110. Redza-Dutordoir M, Averill-Bates DA. Activation of apoptosis signalling pathways by reactive oxygen species. *Biochim Biophys Acta*. 2016;1863(12):2977-2992. doi:10.1016/j.bbamcr.2016.09.012
111. Chen HW, Huang XD, Li HC, et al. Expression of FOXJ1 in hepatocellular carcinoma: correlation with patients' prognosis and tumor cell proliferation. *Mol Carcinog*. 2013;52(8):647-659. doi:10.1002/mc.21904
112. Chen HM, Wu YC, Chia YC, et al. Gallic acid, a major component of *Toona sinensis* leaf extracts, contains a ROS-mediated anti-cancer activity in human prostate cancer cells. *Cancer Lett*. 2009;286(2):161-171. doi:10.1016/j.canlet.2009.05.040
113. Choubey S, Varughese LR, Kumar V, Beniwal V. Medicinal importance of gallic acid and its ester derivatives: a patent review. *Pharm Pat Anal*. 2015;4(4):305-315. doi:10.4155/ppa.15.14
114. Yadav A, Lomash V, Samim M, Flora SJ. Curcumin encapsulated in chitosan nanoparticles: a novel strategy for the treatment of arsenic toxicity. *Chem Biol Interact*. 2012;199(1):49-61. doi:10.1016/j.cbi.2012.05.011
115. Kakkar V, Kaur IP. Evaluating potential of curcumin loaded solid lipid nanoparticles in aluminium induced behavioural, biochemical and histopathological alterations in mice brain. *Food Chem Toxicol*. 2011;49(11):2906-2913. doi:10.1016/j.fct.2011.08.006
116. Abdel-Aziz MS, Shaheen MS, El-Nekeety AA, Abdel-Wahhab MA. Antioxidant and antibacterial activity of silver nanoparticles biosynthesized using *Chenopodium murale* leaf extract. *J Saudi Chem Soc*. 2014;18(4):356-363.
117. Zhu XD, Tang ZY, Sun HC. Targeting angiogenesis for liver cancer: past, present, and future. *Genes Dis*. 2020;7(3):328-335. doi:10.1016/j.gendis.2020.03.010
118. Gupta K, Kshirsagar S, Li W, et al. VEGF Prevents apoptosis of human microvascular endothelial cells via opposing effects on MAPK/ERK and SAPK/JNK signaling. *Exp Cell Res*. 1999;247(2):495-504. doi:10.1006/excr.1998.4359
119. Zhao B, Hu M. Gallic acid reduces cell viability, proliferation, invasion and angiogenesis in human cervical cancer cells. *Oncol Lett*. 2013;6(6):1749-1755. doi:10.3892/ol.2013.1632
120. Zhong XS, Liu LZ, Skinner HD, Cao Z, Ding M, Jiang BH. Mechanism of vascular endothelial growth factor expression mediated by cisplatin in human ovarian cancer cells. *Biochem Biophys Res Commun*. 2007;358(1):92-98. doi:10.1016/j.bbrc.2007.04.083
121. Nath D, Banerjee P. Green nanotechnology—a new hope for medical biology. *Environ Toxicol Pharmacol*. 2013;36(3):997-1014. doi:10.1016/j.etap.2013.09.002
122. Zhang Y, Li M, Gao X, Chen Y, Liu T. Nanotechnology in cancer diagnosis: progress, challenges and opportunities. *J Hematol Oncol*. 2019;12(1):137. doi:10.1186/s13045-019-0833-3
123. Cersosimo RJ. Hepatotoxicity associated with cisplatin chemotherapy. *Ann Pharmacother*. 1993;27(4):438-441. doi:10.1177/106002809302700408
124. Monier A, Guiu B, Duran R, et al. Liver and biliary damages following transarterial chemoembolization of hepatocellular carcinoma: comparison between drug-eluting beads and lipiodol emulsion. *Eur Radiol*. 2017;27(4):1431-1439. doi:10.1007/s00330-016-4488-y
125. Cheng S, Yu X, Liu S, et al. Development of a prognostic nomogram in hepatocellular carcinoma with portal vein tumor thrombus following trans-arterial chemoembolization with drug-eluting beads. *Cancer Manag Res*. 2021;13:9367-9377. doi:10.2147/CMAR.S341672
126. Fu Y, Cai J, Li F, et al. Chronic effects of repeated low-dose cisplatin treatment in mouse kidneys and renal tubular cells [published correction appears in *Am J Physiol Renal Physiol*. 2022 Feb 1;322(2):f193-F194]. *Am J Physiol Renal Physiol*. 2019;317(6):F1582-F1592.
127. de Albuquerque Wanderley Sales V, Timóteo TRR, da Silva NM, et al. A systematic review of the anti-inflammatory effects of gallium compounds. *Curr Med Chem*. 2021;28(10):2062-2076. doi:10.2174/0929867327666200525160556
128. Dong J, Fang D, Zhang L, Shan Q, Huang Y. Gallium-doped titania nanotubes elicit anti-bacterial efficacy in vivo against *Escherichia coli* and *Staphylococcus aureus* biofilm. *Materialia*. 2019;5:100209.
129. Epstein H, Berger V, Levi I, et al. Nanosuspensions of alendronate with gallium or gadolinium attenuate neointimal hyperplasia in rats. *J Control Release*. 2007;117(3):322-332. doi:10.1016/j.jconrel.2006.10.030
130. Abdel-Daim MM, Khalil SR, Awad A, Abu Zeid EH, El-Aziz RA, El-Serehy HA. Ethanolic extract of *Moringa oleifera* leaves influences NF- $\kappa$ B signaling pathway to restore kidney tissue from cobalt-mediated oxidative injury and inflammation in rats. *Nutrients*. 2020;12(4):1031. doi:10.3390/nu12041031
131. Narayanasamy P, Switzer BL, Britigan BE. Prolonged-acting, multi-targeting gallium nanoparticles potently inhibit growth of both HIV and mycobacteria in co-infected human macrophages [published correction appears in *Sci Rep*. 2021 Sep 1;11(1):17757]. *Sci Rep*. 2015;5(1):1-7. doi:10.1038/srep08824
132. Lima KG, Krause GC, Schuster AD, et al. Gallic acid reduces cell growth by induction of apoptosis and reduction of IL-8 in HepG2 cells. *Biomed Pharmacother*. 2016;84:1282-1290. doi:10.1016/j.biopha.2016.10.048
133. Yaegashi A, Yoshida K, Suzuki N, et al. A case of severe hepatotoxicity induced by cisplatin and 5-fluorouracil. *Int Cancer Conf J*. 2019;9(1):24-27. doi:10.1007/s13691-019-00394-2